Phil. Trans. R. Soc. Lond. B **324**, 149–172 (1989) [149]
Printed in Great Britain

AUTOTOMY OF CERATA BY THE NUDIBRANCH *MELIBE LEONINA* (MOLLUSCA): ULTRASTRUCTURE OF THE AUTOTOMY PLANE AND NEURAL CORRELATE OF THE BEHAVIOUR

BY LOUISE R. BICKELL-PAGE
Department of Biology, University of Victoria, Victoria, British Columbia, Canada, V8W 2Y2

(*Communicated by Q. Bone, F.R.S. – Received* 1 *September* 1988)

[Plates 1–8]

CONTENTS

A strong aversive stimulus, such as a firm pinch, to a ceras of the nudibranch mollusc *Melibe leonina*, is both necessary and sufficient to cause autotomy (rapid severance) of the ceras at a predictable site at its base (autotomy plane). Ceratal autotomy, in concert with swimming behaviour, may be a means of escaping crab predators.

Cerata are innervated by ceratal nerves, which branch from the pleural nerves. Within each ceras, the corresponding ceratal nerve extends to a variable number of peripheral ceratal ganglia and an offshoot runs to two interconnected nerve rings within the ceratal autotomy plane. The nerve rings and their connectives contain innervated granule-filled cells. (GCs) that are morphologically distinct from gliointerstitial cells. Cytoplasmic processes of GCs impinge onto the basal laminae and associated connective tissue fibrils of the four structures that cross the autotomy

plane: epidermis, digestive gland, longitudinal muscle bands and ceratal nerve. The distribution of GCs and their degranulation during autotomy suggests a role in the autotomy mechanism.

Ceratal autotomy is accompanied by strong contraction of sphincter muscles flanking the autotomy plane and of longitudinal muscle bands within the ceras. Muscle contraction appears to assist in the autotomy mechanism by placing tensile stress on tissues at the level of the autotomy plane. Wound closure following autotomy is effected by contraction of the sphincter muscles.

Extracellular recordings from nerves emanating from ceratal peripheral ganglia show a long-lasting train of large amplitude, compound spike bursts following an aversive stimulus to the ceratal epidermis or a suprathreshold stimulus to a nerve entering a peripheral ganglion. The patterned output precedes ceratal autotomy. Intracellular recordings from ceratal ganglia suggest that the patterned output is generated by a group of ganglion cells (synchronous response (SR) neurons) that fire synchronously. I argue that SR neurons are efferents to ceratal muscles and that SR neurons participate in ceratal autotomy by signalling strong, synchronous contractions of these muscles.

Introduction

Autotomy was defined by Frédéricq (1883) as the ability to detach a body part rapidly after the part receives a threatening stimulus. This dramatic behaviour may allow escape from predators, as demonstrated for tail autotomy by lizards (see Congdon *et al.* 1974; Dial & Fitzpatrick 1983). Despite the many examples of autotomy by molluscs (Stasek 1967), and the extensive use of molluscs for research on the neural control of behaviour (see Kandel 1976, 1979), almost nothing is known of the mechanism or control of autotomy in this phylum.

Structural characteristics enabling rapid detachment of an appendage and subsequent wound closure have been documented most thoroughly for the Echinodermata (see reviews by Emson & Wilkie (1980) and Wilkie (1984)), Arthropoda (see reviews by McVean (1975, 1982)), and Chordata (see Wake & Dresner 1967; Sheppard & Bellairs 1972). The physiological control of autotomy has been best studied for the walking limbs of brachyuran crabs. McVean (1974) and McVean & Findlay (1976) identified a unique orchestration of neural activity that directs limb muscles to break cuticular specializations at the base of the leg. Among echinoderms, arm autotomy by brittlestars appears to be under direct neural control (Wilkie 1978*b*), where evisceration by sea cucumbers may also involve a substance (possibly neurosecretory) released into the coelom (Smith & Greenberg 1973; Byrne 1986).

The cerata of many nudibranch and sacoglossan gastropods can separate quickly and cleanly from the dorsal body wall following an aversive stimulus (Kress 1968; Jensen 1984; earlier literature reviewed by Stasek (1967)). The short time interval between an adequate stimulus and the autotomy response superficially suggests neural control of the behaviour. Neurophysiological studies have shown that various appendages of molluscs are under dual or interactive control by ganglia of the central nervous system (CNS) and by peripheral neurons situated along peripheral nerves (Prior 1972*a*, *b*; Lukowiak & Jacklet 1972, 1975; Peretz *et al.* 1976; Bailey *et al.* 1979; Perlman 1979). Therefore investigation of the control of ceratal autotomy must consider a possible role by peripheral neurons within the ceras.

Using behavioural observations, electron microscopy and neurophysiological methods, I studied the mechanism and peripheral neural control of ceratal autotomy in the dendronotid nudibranch *Melibe leonina* (Gould, 1852). Dense populations of this large nudibranch occur within eelgrass and kelp beds along the west coast of North America. *M. leonina* is recognized

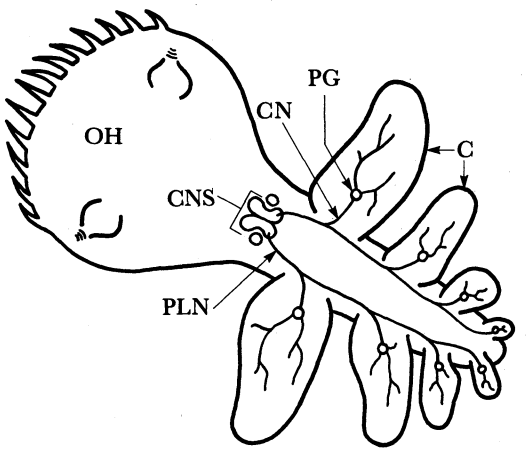

FIGURE 1. Sketch of adult *Melibe leonina* in dorsal view showing oral hood (OH) and cerata (C). Ceratal nerves (CN) arise from the pleural nerves (PLN) that extend from the CNS. Primary ceratal ganglion (PG).

by its large oral hood, used to engulf small planktonic and epiphytic crustaceans (see Agersborg 1921; Hurst 1968; Ajeska & Nybakken 1976), and by two rows of large, petaloid cerata arranged in order of decreasing size along the dorsum (figure 1).

MATERIALS AND METHODS

Adult specimens of *Melibe leonina* measuring approximately 5 cm in relaxed foot length were collected from the eelgrass bed in Patricia Bay, Vancouver Island, Canada, by SCUBA divers. Juveniles having a foot length of approximately 0.5 cm were reared in the laboratory (see Bickell & Kempf 1983) from egg masses also collected from Patricia Bay.

(*a*) *Electron microscopy*

Before fixation, animals were anaesthetized in an artificial seawater solution containing an excess of Mg^{2+} and reduced Ca^{2+} (recipe according to Audesirk & Audesirk (1980)). Portions of body wall cut from the base of adult cerata were pinned to a small block of Sylgard (Dow-Corning) before being immersed in primary fixative for 5 h at room temperature. Juveniles were fixed whole for 5 h. The primary fixative consisted of glutaraldehyde (2.5% by volume) in 0.2 M phosphate buffer (pH 7.6) with NaCl added to make the fixative isosmotic with seawater (Cloney & Florey 1968). After several rinses in sodium bicarbonate (25 g l^{-1}) (pH 7.2), specimens were placed in osmium tetroxide (20 gl^{-1}) diluted in sodium bicarbonate (12.5 g l^{-1}) for 1 h. Ethanol dehydration and infiltration with Epon 812 followed standard procedure (Luft 1961). Thin sections were stained for 20 min at 60 °C in aqueous uranyl acetate, followed by 10 min at room temperature in lead citrate, and photographed with a Philips EM300 transmission electron microscope.

The small size of juveniles, relative to adults, facilitated structural reconstruction of the ceratal autotomy plane from serial sections. Therefore a series of sections through the entire, intact autotomy plane of a juvenile ceras was prepared by cutting one to three 1 μm sections alternating with five to seven grids of thin sections (ceras oriented longitudinally). The basic structure of the autotomy plane revealed by this specimen was confirmed by examining thin

sections through selected regions of ceratal autotomy plane in several other juveniles and in adults. All electronmicrographs shown in this paper were taken from juveniles.

Autotomized cerata for ultrastructural observations were obtained by pinching juvenile cerata to induce autotomy before fixation according to the procedure outlined above.

(*b*) *Neurophysiology*

Animals for neurophysiological experiments were held in the flow-through seawater system at Friday Harbor Laboratories, University of Washington, U.S.A. Holding temperatures varied between 9 and 12 °C. Three types of preparation were used for neurophysiological recordings: isolated ceras, isolated primary ceratal ganglion with attached nerve trunks, and whole animal with ganglia of the CNS removed.

Isolated cerata were pinned to a layer of Sylgard in a petri dish and opened by a cut extending from the base to halfway down the midline of the lateral face. Nerves and ganglia were exposed by carefully removing attached connective tissue and the petri dish was immersed in a chamber that received a continuous flow of seawater. Extracellular electrodes held by micromanipulators were attached to various nerves within the ceras as described in the Results.

Intracellular recordings were made from primary ceratal ganglia that were removed from cerata along with lengthy portions of the ceratal nerve and several distal nerves (see figure 2). This was secured with cactus (*Opuntia* sp.) spines to a Sylgard-lined petri dish and the filtered seawater surrounding the preparation was periodically replaced.

Whole animals with central ganglia removed were prepared for extracellular recordings from a distal nerve within a ceras as described in the Results. Like isolated cerata, each whole animal preparation was continuously irrigated with seawater.

Extracellular suction electrodes were made by drawing out polyethylene tubing. Intracellular electrodes were made from glass microcapillary tubes having a glass filament within the lumen, were filled with 3 M KCl, and had resistances of 50–100 MΩ. Neural activity recorded by intracellular and extracellular electrodes was amplified and displayed according to conventional techniques.

Tactile stimuli were applied to the ceratal epidermis with a glass probe mounted on a micromanipulator. Individual seastar tube feet were slipped over the shaft of a polyethylene electrode, secured by suction, and touched to the ceratal epidermis with the aid of a micromanipulator. Cerata were pinched with hand-held forceps. Electrical stimuli to various nerves within the ceras were applied via polyethylene suction electrodes using a stimulator and stimulus isolation unit.

Results

(*a*) *Autotomy behaviour*

When a ceras of *M. leonina* is pinched firmly with forceps, the base of the ceras becomes greatly constricted because of strong contractions of sphincter muscles in this region. Although less obvious, longitudinal muscles within the ceras also contract. Usually within 10 s of an adequate stimulus, the base of the ceras separates cleanly from the dorsal body wall. Neighbouring cerata do not autotomize unless also pinched firmly and pinches given to other body parts, including non-ceratal sites on the dorsum, do not induce basal constriction or autotomy of cerata. A moderate-intensity pinch to a ceras may fail to cause its autotomy, but the ceratal muscles still contract. Autotomized cerata show little spontaneous movement.

Although cerata of *M. leonina* narrow towards their base, the ceratal autotomy plane is not inherently fragile. Considerable force is needed to tear cerata from animals anaesthetized for 36 h in high Mg^{2+}, low Ca^{2+}, artificial seawater.

Pinching a ceras of *M. leonina* also causes the whole animal to contract and eventually releases the swimming behaviour described by Hurst (1968). Swimming may begin before or after actual separation of the ceras. On several occasions, I observed *M. leonina* (5 cm relaxed foot length) escape from a small predatory crab (2.0–3.0 cm carapace width) by autotomizing one or more cerata held by the chela of the crab. Swimming by the nudibranch then carried it beyond the grasp of the crab.

Contact by predatory seastars such as *Pycnopodia helianthoides* does not induce ceratal autotomy by *M. leonina* and, unlike the dendronotid nudibranchs *Tritonia diomedea* and *Dendronotus frondosus* (Mauzey *et al.* 1968), does not usually induce swimming by *M. leonina*. The typical response of *M. leonina* to contact by *Pycnopodia* is general body contraction often followed by a variable period of 'galloping', a method of rapid pedal locomotion (Agersborg 1923). *M. leonina* is protected from most seastars by a defensive chemical released from subepidermal repugnatorial glands that is not effective against crabs (Ajeska & Nybakken 1976; Page 1988).

Populations of *M. leonina* were sampled to determine the extent of ceratal losses in the field. Two samples of 41 and 81 animals, respectively, were collected from different locations around southern Vancouver Island at different times of year. Sixty-five (53.3%) of the 122 animals were in the process of regenerating lost cerata and 35 of these had more than one regenerative bud.

(*b*) *Structure of intact autotomy plane*

(i) *General*

As illustrated in figure 2, four structures extend across the autotomy plane at the base of each ceras and therefore must be broken during autotomy: the epidermis, a branch of the digestive gland, the ceratal nerve that arises from the ipsilateral pleural nerve, and longitudinal muscle bands that originate within the dorsum of the body (proximal to the autotomy plane) and insert near the apex of the ceras. Although the digestive gland and ceratal nerve eventually undergo extensive branching within each ceras, they both enter as a single undivided trunk. In addition to these four structures, the complex system of fluid-filled haemal sacs, which constitutes the hydraulic skeleton of *M. leonina*, extends from the body into each ceras.

A pair of sphincter muscles flank the autotomy plane, immediately beneath the ceratal epidermis and superficial to the longitudinal muscle bands (figure 2). A second pair of sphincter muscles surrounds the digestive gland, also on either side of the autotomy plane. Occasional circular muscles are present between the subepidermal and digestive gland sphincters.

(ii) *Ceratal muscles: ultrastructure*

The subepidermal and digestive gland sphincter muscles and the longitudinal muscle bands are each composed of a staggered array of muscle cells that lack an obvious cross or oblique alignment of Z bodies. Connective-tissue fibrils invest individual muscle cells of each sphincter and longitudinal muscle band (figures 3 and 4†). Although the fibrils are probably some form of collagen, they measure only 12–15 nm in diameter and are not obviously banded.

† Figures 3–6 and 8–23 appear on plates 1–8.

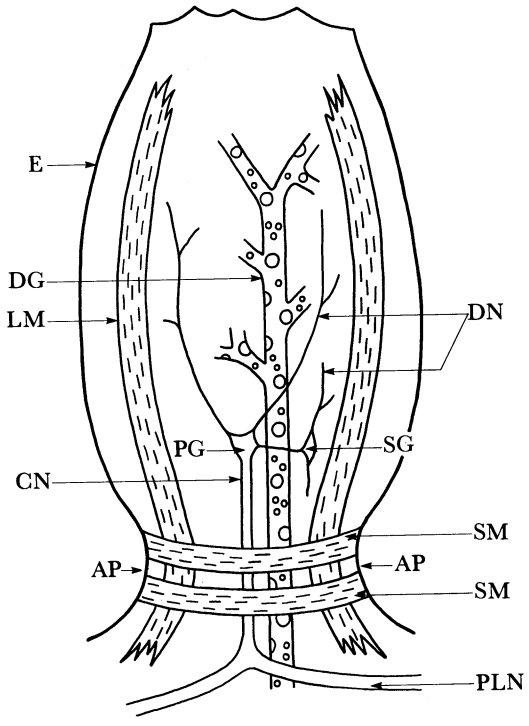

FIGURE 2. Sketch of a ceras showing structures that cross the autotomy plane (AP): epidermis (E), digestive gland (DG), longitudinal muscle bands (LM), and ceratal nerve (CN) extending from pleural nerve (PLN). Subepidermal sphincter muscles (SM) flank the autotomy plane (digestive gland sphincters not shown). Primary and secondary ceratal ganglia (PG and SG, respectively) give rise to distal nerves (DN). Drawing not to scale.

Hemifasciae adherentes occur frequently along the sarcolemma of the muscle cells (figures 3, 4 and 5). Like hemidesmosomes, hemifasciae adherentes are discontinuous junctional complexes, but actin-containing thin filaments, rather than intermediate filaments, insert on the sarcoplasmic side of the membrane specialization (figure 5). Direct junctional complexes (fasciae adherentes) between neighbouring muscle cells were occasionally observed (figure 4).

On either side of the autotomy plane, concentrations of connective tissue fibrils, presumably representing attachment sites, are located between the subepidermal sphincter muscles and the ceratal epidermis (figure 3), and between the sphincters and the longitudinal muscle bands (figure 5). The latter pass close to the two subepidermal sphincter muscles while extending from the dorsum into the ceras.

Small bundles of axons lie alongside the sphincter muscles and longitudinal muscle bands and neuromuscular synapses were frequently found (figure 6).

(iii) *Autotomy plane nerve rings and granule-filled cells*

Two nerve rings are located within the ceratal autotomy plane (figure 7): the subepidermal nerve ring encircles the base of the ceras immediately beneath the ceratal epidermis, and the digestive gland nerve ring surrounds the digestive gland. The subepidermal nerve ring lies between the two subepidermal sphincter muscles (figure 8), and the digestive gland nerve ring lies between the two digestive gland sphincters. The two nerve rings are linked by connectives and are extensions of a branch of the ceratal nerve. The branch arises from the ceratal nerve on the distal (ceratal) side of the autotomy plane (figure 7).

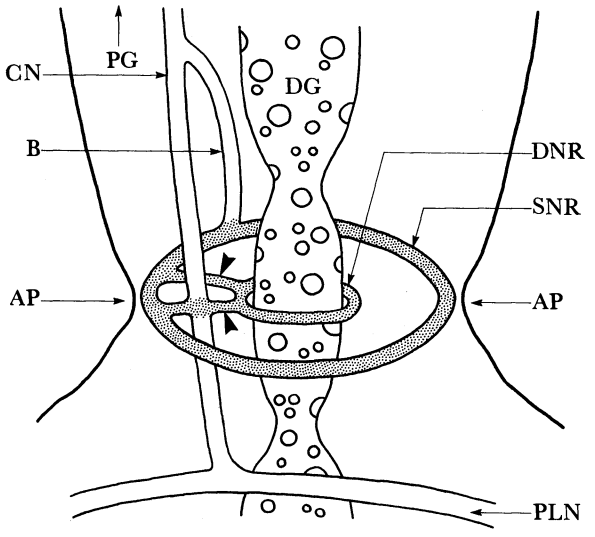

FIGURE 7. Sketch of nerve tracts associated with ceratal autotomy plane (AP) in a juvenile *M. leonina*. A branch (B) of the ceratal nerve (CN) gives rise to a subepidermal nerve ring (SNR) that is linked by connectives (arrowheads) to a second nerve ring (DNR) encircling the digestive gland (DG). Stippling identifies nerve tracts that contain granule-filled cells. Primary ceratal ganglion (PG); pleural nerve (PLN). Drawing not to scale.

Somata and cytoplasmic processes of many, distinctive granule-filled cells (GCs) are contained within the perineurium of the two nerve rings and the connectives between them (figure 8). Each GC contains a large nucleus with prominent nucleolus and the perinuclear cytoplasm contains mitochondria, polyribosomes, smooth and rough endoplasmic reticulum and several Golgi bodies. The Golgi give rise to primary vesicles containing an electron-dense material (figure 9) that appear to be precursors of the larger (mean diameter = 180 nm; maximum diameter = 280 nm; $n = 56$) membrane-bounded dense granules that are characteristic of this cell type (figures 9, 10 and 11). Most of the mature granules occur within cytoplasmic processes of GCs, where smooth endoplasmic reticulum is also abundant (figure 10).

Axons of the autotomy plane nerve rings show occasional interaxonal synapses but most of the synaptic profiles I observed were onto somata and cytoplasmic processes of GC (figure 11).

The granules within GCs are smaller and morphologically distinct from the granules of gliointerstitial cells associated with muscle cells of the sphincters and longitudinal muscle bands and with small groups of axons that occur adjacent to these muscles (compare figures 11 and 12). A detailed review of the structure, distribution and cytochemistry of gliointerstitial cells within molluscs has been given by Nicaise (1973). The granules of gliointerstitial cells are larger (mean diameter of granular core = 370 nm; maximum diameter = 730 nm; $n = 53$) than those of GCs, and gliointerstitial granules in my tissue sections consistently show irregular swelling of the limiting membrane away from the granular product (figure 12).

As described below, granule-filled cytoplasmic processes of GCs are associated with the basal laminae and investing connective tissue fibrils of the four structures that cross the ceratal autotomy plane, and the contacts occur only in the restricted region of the autotomy plane. Sections taken from random sites along the length of cerata, the dorsum and the periphery of the oral hood contained profiles of gliointerstitial cells but not of GCs.

Figure 10 shows granule-filled processes of GCs extending from the subepidermal nerve ring

(where GC cells bodies are located) towards the ceratal epidermis. Contacts between processes of GCs and the basal lamina of the ceratal epidermis occur virtually uninterrupted along the entire epidermal autotomy plane circumscribing the base of the ceras.

Each longitudinal muscle band actually penetrates through the subepidermal nerve ring where the bands extend from the dorsum of the body into the ceras (figure 13). At the level of penetration, granule-filled processes of GCs interdigitate with the individual muscle cells of the longitudinal muscle bands and their associated connective tissue fibrils (figures 14 and 15). However, GC processes do not infiltrate the connective tissue attachments between the longitudinal muscle bands, the subepidermal sphincter muscles and the epidermides that occur on either side of the ceratal autotomy plane.

Figure 16 shows one of the connectives between the subepidermal and digestive gland nerve rings. Cross sections through the digestive-gland nerve ring show that cell bodies of GCs are located within this axon bundle and granule-filled cytoplasmic processes of GCs impinge on the basal lamina and associated connective tissue fibrils of the digestive cells (figure 17).

The ceratal nerve crosses the autotomy plane in the mid-region of the lateral side of the ceras. At the point of intersection, the ceratal nerve forms an anastomosis with one of the connectives extending between the two autotomy-plane nerve rings (figure 18). Processes of GCs are closely applied to the perineurium of the ceratal nerve in the area of the anastomosis (figure 19).

(*c*) *Structure of broken autotomy plane*

After ceratal autotomy, tissues within the base of the ceras are crowded together (figure 20) because of contraction of muscles in the area. The subepidermal sphincter muscle and the broken ends of the longitudinal muscle bands (on the ceratal side of the autotomy plane) border on a large bundle of axons that lies immediately beneath the area of ceratal epidermis that has detached from the dorsal body wall of the nudibranch. The position of this axonal

---

Description of plate 1

Figure 3. Cross section through subepidermal sphincter muscle (SM) showing arrays of connective-tissue fibrils (asterisks) between muscle fibres and between the muscle and ceratal epidermis (E). Hemifasciae adherentes (large arrowheads); hemidesmosome (small arrowhead).

Figure 4. Longitudinal muscle band (LM), where it bypasses a subepidermal sphincter muscle (SM), showing concentrations of connective tissue fibrils (asterisks) between the two muscle groups. Hemifasciae adherentes (large arrowheads); fasciae adherentes (small arrowheads).

Figure 5. Hemifascia adherens (demarcated by arrowheads) of a longitudinal muscle fibre (LM). Arrows indicate thin myofilaments.

Figure 6. Neuromuscular synapse (demarcated by arrowheads) onto a longitudinal muscle fibre (LM).

Description of plate 2

Figure 8. Section through the ceratal autotomy plane (AP) showing the epidermis (E), subepidermal nerve ring (SNR), and the two subepidermal sphincter muscles (SM). The nucleus of a granule-filled cell is marked by an asterisk.

Figure 9. Perinuclear cytoplasm of a GC. Primary vesicles (arrowheads) produced by the Golgi (G) give rise to characteristic granules (GR) of these cells. Nucleus (N).

Figure 10. Cellular processes of GC impinging on the basal lamina (asterisks) of the ceratal epidermis (E). Arrowheads indicate smooth endoplasmic reticulum.

Figure 11. Synapse (demarcated by arrowheads) onto a GC.

Figure 12. Granules of a gliointerstitial cell.

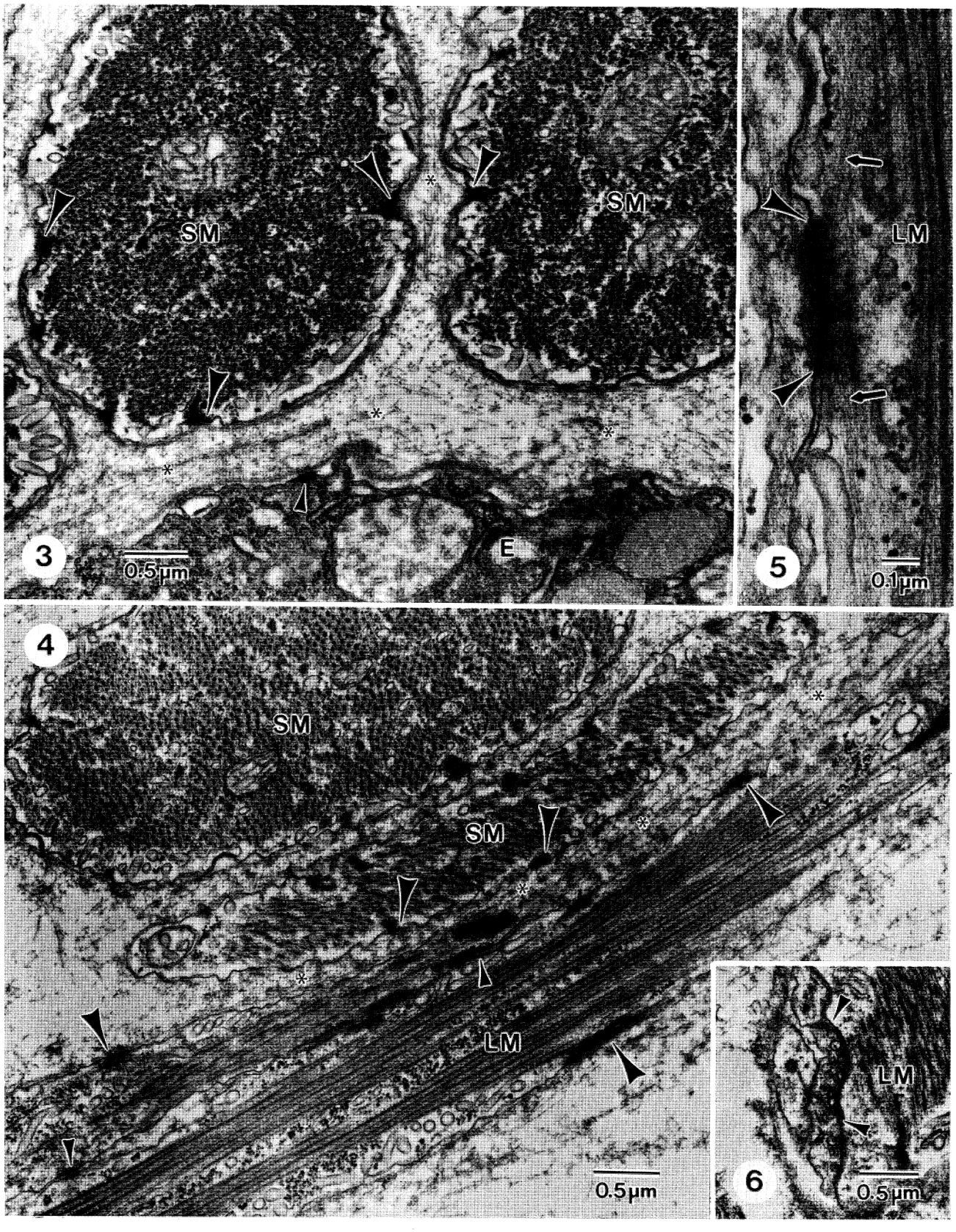

FIGURES 3–6. For description see opposite.

(*Facing p.* 156)

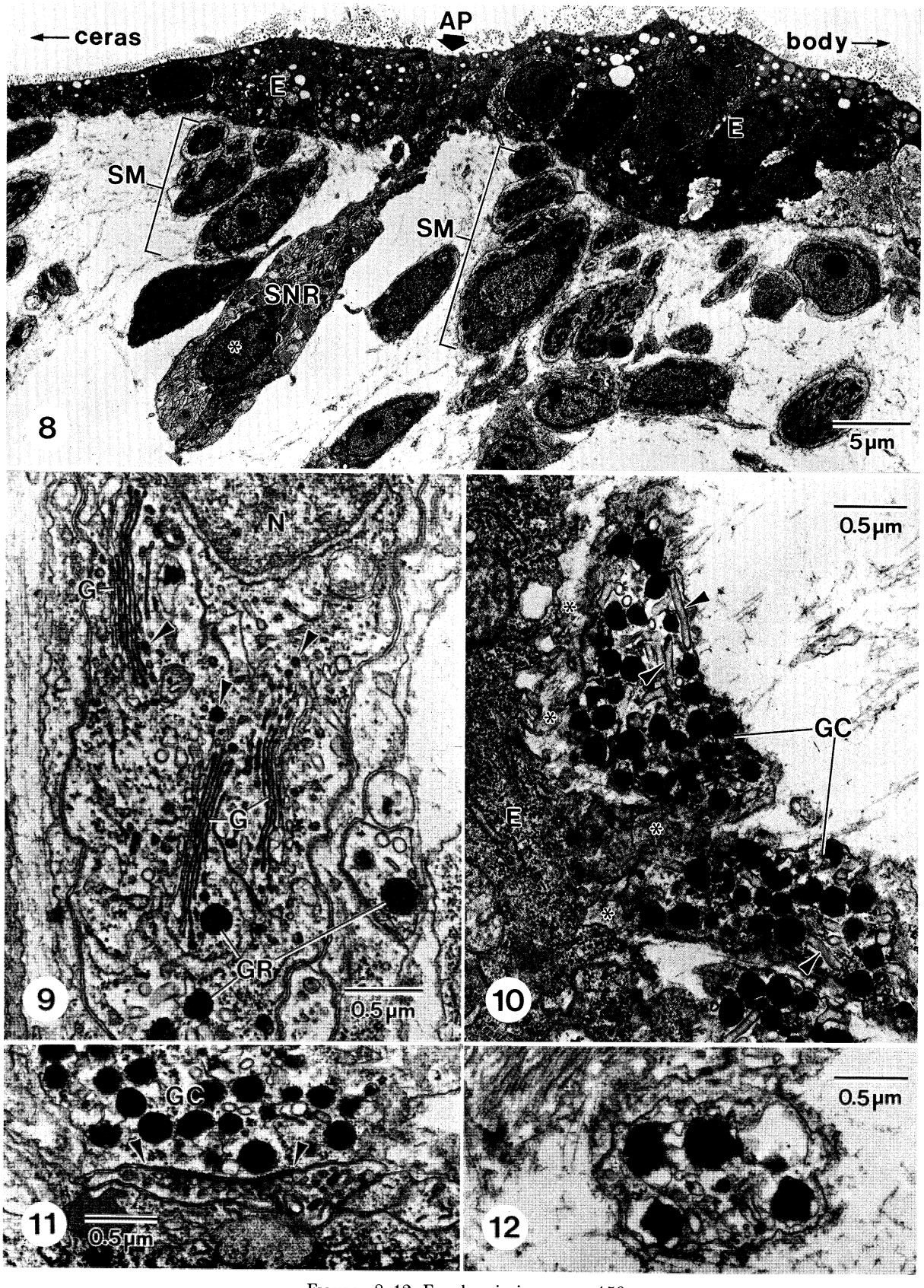

FIGURES 8–12. For description see p. 156.

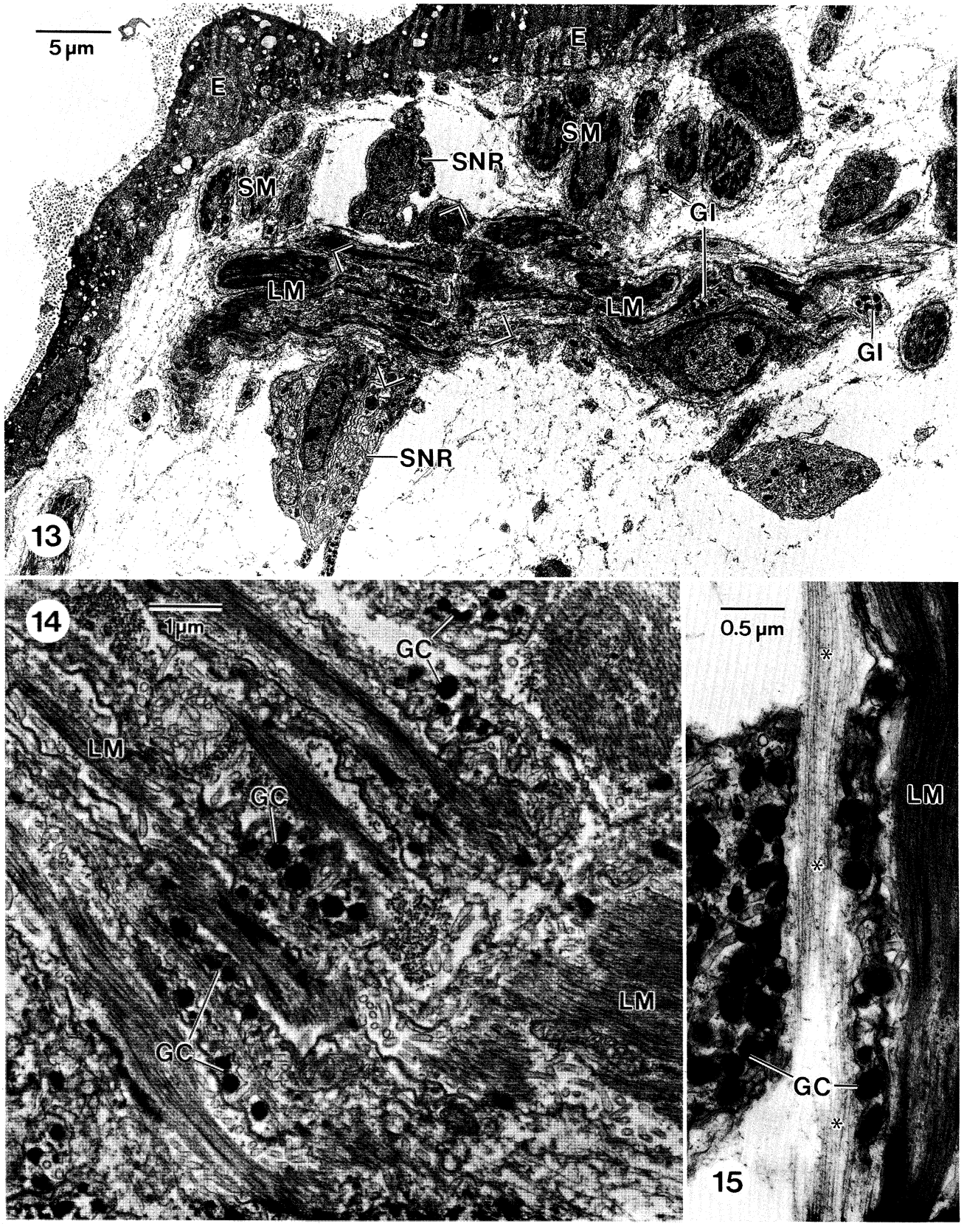

FIGURE 13. Longitudinal section through a longitudinal muscle band (LM) penetrating the subepidermal nerve ring (SNR). Epidermis (E); gliointerstitial cell processes (GI); subepidermal sphincter muscles (SM). Enlargement of bracketed area is shown in figure 14.

FIGURE 14. Cellular processes of granule-filled cells (GC) interdigitating with longitudinal-muscle fibres (LM) within the autotomy plane.

FIGURE 15. Detail of GC processes impinging onto a longitudinal-muscle fibre (LM) and associated connective tissue fibrils (asterisks).

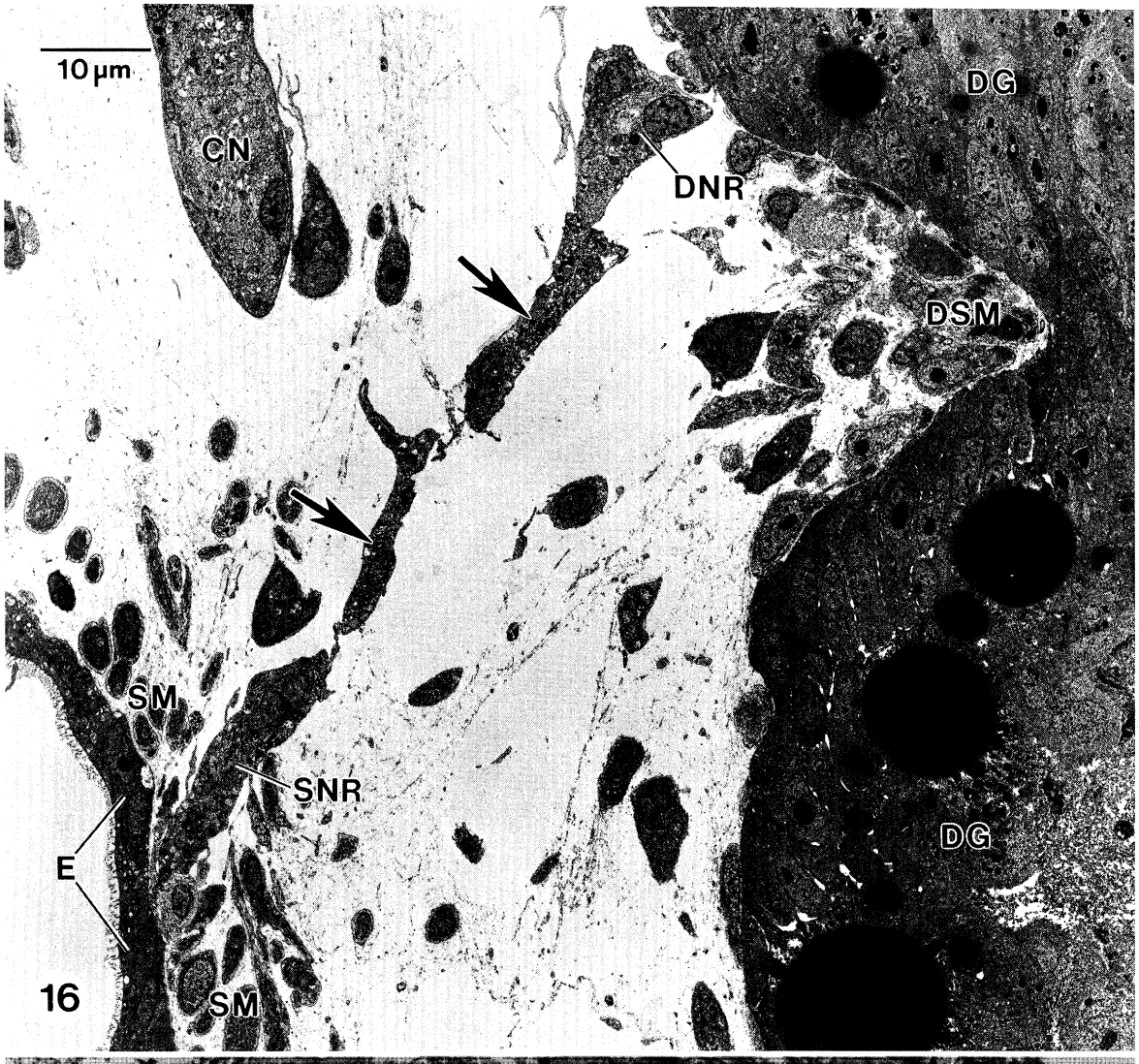

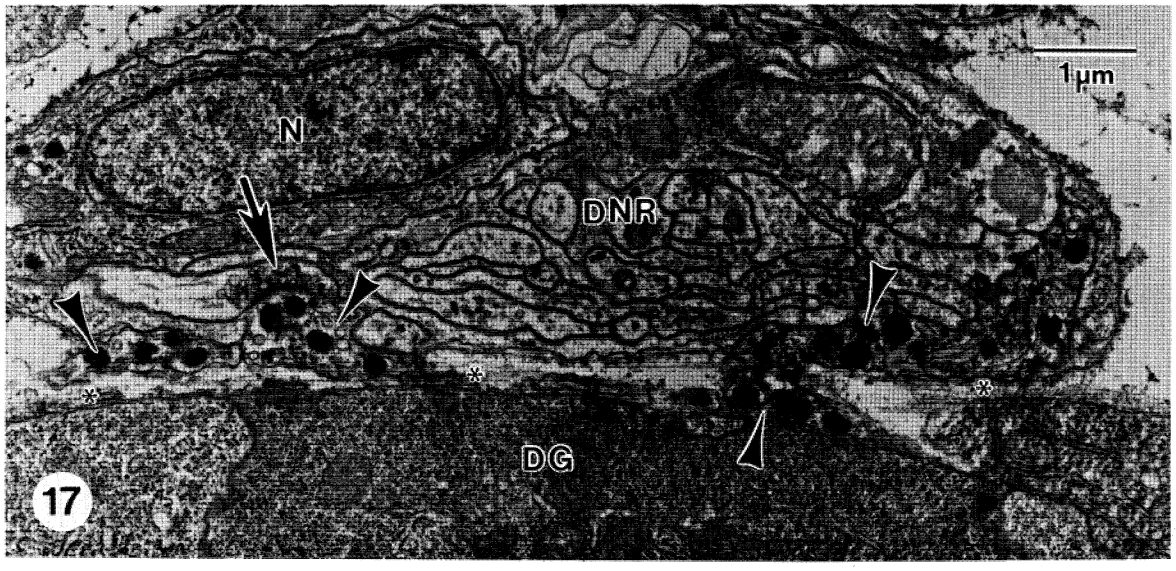

FIGURE 16. Longitudinal section through the ceratal autotomy plane showing one of the connectives (arrows) extending between the subepidermal nerve ring (SNR) and the digestive-gland nerve ring (DNR). Ceratal nerve (CN), digestive gland (DG), digestive-gland sphincter muscle (DSM), epidermis (E), subepidermal sphincter muscles (SM).

FIGURE 17. Cross section through the digestive gland nerve ring (DNR) showing the nucleus (N) of a GC and cellular processes of GC (arrowheads) impinging onto the basal lamina and connective tissue fibrils (asterisks) of the digestive gland (DG). The arrow indicates a synapse onto a GC process.

FIGURE 18. Oblique section through the ceratal nerve (CN) where it forms an anastomosis with a connective (CO) between the subepidermal nerve ring (SNR) and the digestive-gland nerve ring. Note the cell body of a GC. Epidermis (E).

FIGURE 19. Cytoplasmic processes of GC (large arrows) associated with the perineurium (small arrows) of the ceratal nerve (CN).

FIGURE 20. Longitudinal section through the base of an autotomized ceras. The broken ends of the longitudinal muscle bands (LM), epidermis (E), and digestive gland (DG) are indicated by arrows labelled 1, 2 and 3, respectively. Also note contracted digestive-gland sphincter (DSM), occasional circular muscles (OC), and subepidermal sphincter muscles (SM), and the subepidermal nerve ring (SNR). The bracketed area is enlarged in figure 21.

FIGURE 21. Longitudinal section through the epidermis (E) and subepidermal structures on the ceratal side of the autotomy plane of an autotomized ceras. Note the disruption (large arrow) of the epidermal basal lamina and associated connective-tissue fibrils (small arrows) just before the terminal epidermal cell (large asterisk) and the paucity of GC granules within the subepidermal nerve ring (SNR). Several granules (arrowheads) are present within a possible GC process (small asterisk) overlying the broken stump of the digestive gland (DG).

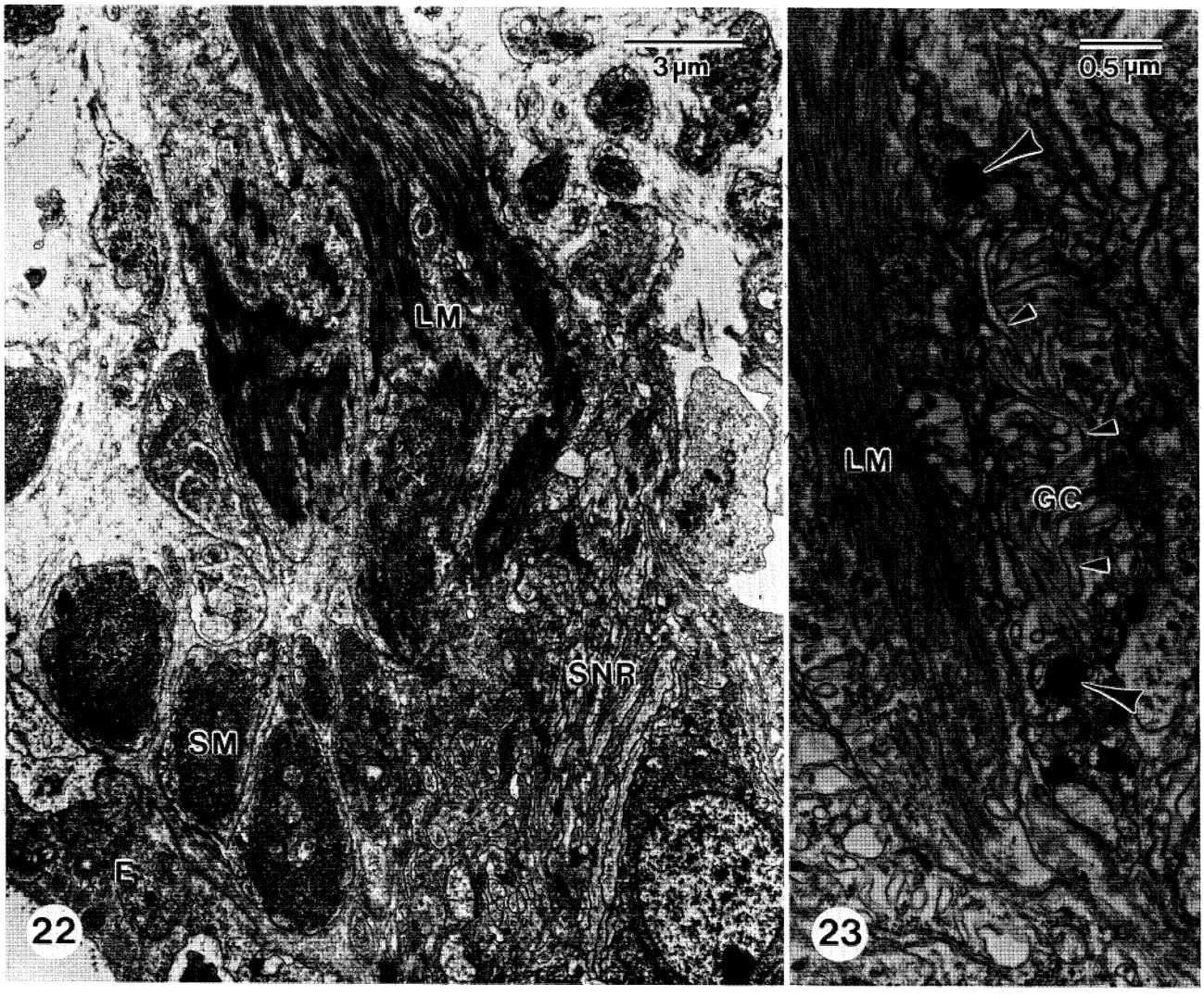

FIGURE 22. Longitudinal section through the base of an autotomized ceras showing the epidermis (E), subepidermal sphincter muscle (SM) and a longitudinal muscle band (LM). The LM is broken where it meets the subepidermal nerve ring (SNR).

FIGURE 23. Cellular process of a possible granule-filled cell (GC) adjacent to a terminal muscle fibre at the broken end of a longitudinal muscle band (LM). The process contains abundant smooth endoplasmic reticulum (small arrowheads) but few dense granules (large arrowheads).

bundle identifies it as the subepidermal nerve ring (figures 20, 21 and 22). However, unlike intact cerata, very few GC granules are associated with the subepidermal nerve ring within autotomized cerata (figures 21 and 22), suggesting that massive degranulation of GC has accompanied autotomy.

The basal lamina underlying the ceratal epidermis is clearly recognizable up to and including the level of the ceratal subepidermal sphincter muscle (figure 21). Beyond the sphincter, a rim of only one or two epidermal cells is retained by the detached ceras. These epidermal cells, which overlie the degranulated subepidermal nerve ring, are noteworthy because they lack a basal lamina (figure 21).

The longitudinal muscle bands terminate immediately proximal to their association with the subepidermal sphincter muscle (on the ceratal side of the autotomy plane; figures 20 and 22) and the sphincter remains bound by connective tissue to the broken ends of the longitudinal muscle bands and to the overlying epidermis. Dissections of autotomized cerata confirm the maintenance of these physical connections throughout the process of autotomy. Adjacent to the broken ends of the longitudinal muscle bands, I found cytoplasmic profiles that I identified as cellular processes of GCs because of an abundance of smooth endoplasmic reticulum, some rough endoplasmic reticulum and, occasionally, membrane-bounded dense granules similar to GC granules in intact cerata (figure 23).

The detached stump of the digestive gland often protrudes slightly from the epidermal wound following ceratal autotomy and a sphincter muscle corresponding to that on the ceratal side of the autotomy plane constricts the trunk of the digestive gland above the level of detachment (figure 20). Because of the extreme constriction of tissues at the base of autotomized cerata, I was unable to identify positively the digestive-gland nerve ring, as distinct from the subepidermal nerve ring. Nevertheless, in several sections I found presumed processes of GCs, containing some unexocytosed dense granules, alongside the broken end of the digestive gland (figure 21).

(*d*) *Neural correlate of autotomy*

(i) *Organization of ceratal peripheral nervous system*

Cerata of *M. leonina* receive central innervation from the pleural ganglia exclusively. The left and right pleural nerves, after emerging from their respective cerebropleural ganglion (part of the CNS), extend posteriorly beneath the dorsolateral body wall of the nudibranch and sprout sequential branches into each ipsilateral ceras. These branches are the ceratal nerves (figure 1).

As shown in figure 2, each ceratal nerve arrives at a peripheral ganglion after entering the ceras. With few exceptions, this primary ceratal ganglion gives rise to one or more connectives to additional, usually smaller ganglia (secondary ceratal ganglia), often located towards the opposite side of the ceras. All ceratal ganglia give rise to a variable number of distal nerves. I had not discovered the two nerve rings within the ceratal autotomy plane when the neurophysiological experiments were done.

Sensory cells with an apical ciliated dendrite, subepidermal cell body and basal axon are clustered beside the pores of the many repugnatorial glands of the ceras (Page 1988). These were the only ceratal receptors identified by scanning and transmission electron microscopy, although others may exist.

(ii) *Neurophysiology*

Isolated ceras: extracellular recordings. Isolated cerata were used for initial neurophysiological investigation of the ceratal peripheral nervous system, in the hope of identifying unique neural signals following stimuli known to initiate ceratal autotomy.

An extracellular electrode placed on the peripheral, cut end of a distal nerve recorded neural impulses to gentle touches by a glass probe to the ceratal epidermis. Presumably, most, if not all, of this activity is afferent. Simultaneous recordings from two distal nerves during touches lasting 1 s with a glass probe to four widely separated locations on the lateral face of the ceras showed extensive overlap in the sensory fields innervated by distal nerves (figure 24). Responses of distal nerves did not markedly outlast the duration of the touch stimulus and did not show an 'off' response following removal of the touch stimulus.

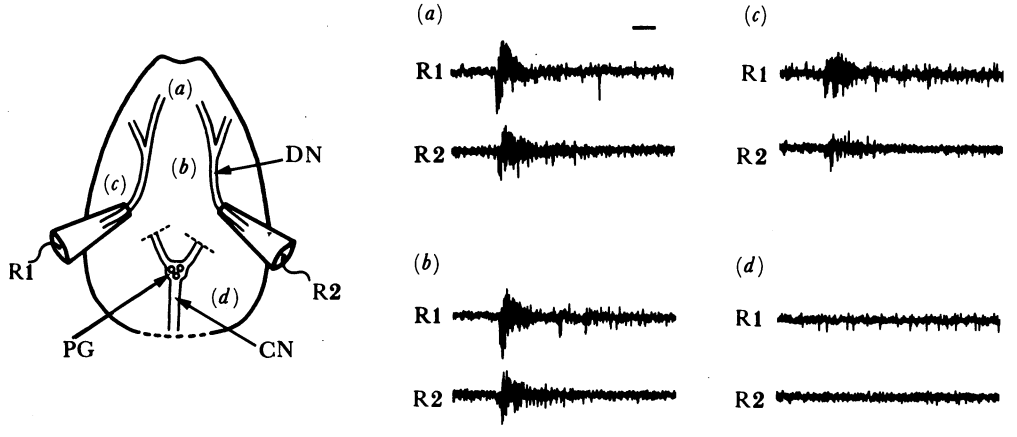

FIGURE 24. Demonstration of extensive overlap in sensory fields innervated by distal nerves. The sketch shows positions of extracellular recording electrodes (R1 and R2) on two distal nerves (DN) during touches lasting 1 s with a glass probe to four different sites (*a–d*) on the ceratal epidermis. The chart traces (*a–d*) show responses to touch at the corresponding sites marked on the diagram. Ceratal nerve (CN); primary ceratal ganglion (PG). Timescale 1 s.

The overlapping sensory fields of distal nerves allowed simultaneous comparison of neural signals entering and leaving the primary ceratal ganglion during epidermal stimulation. As shown in figure 25, one recording electrode (R1) was placed on the peripheral, cut end of a distal nerve and a second recording electrode (R2) was placed on the ceratal nerve as it emerged from the primary ceratal ganglion. Stimuli were applied to the ceratal epidermis in a region likely to give rise to afferent signals within both the cut distal nerve (R1) and intact distal nerves, thereby enabling these signals to be recorded by R1 but also conducted to the primary ceratal ganglion via intact nerves. Figure 25 shows activity recorded from R1 and R2 in response to four different stimuli: a glass probe having a diameter similar to a seastar tube foot (figure 25*a*), a tube foot of the seastar *Pisaster ochraceus* (figure 25*b*), two different touches by a tube foot of the seastar *Pycnopodia helianthoides* (figure 25*c*, *d*), and a firm pinch by forceps to the ceratal epidermis (figure 25*e*).

The response of the distal nerve during each of the four stimuli was a non-patterned train of impulses, although the two *Pycnopodia* tube-foot touches and the pinch (latter not shown in figure 25*e*) produced impulses of higher amplitude than touches by the glass probe or the tube

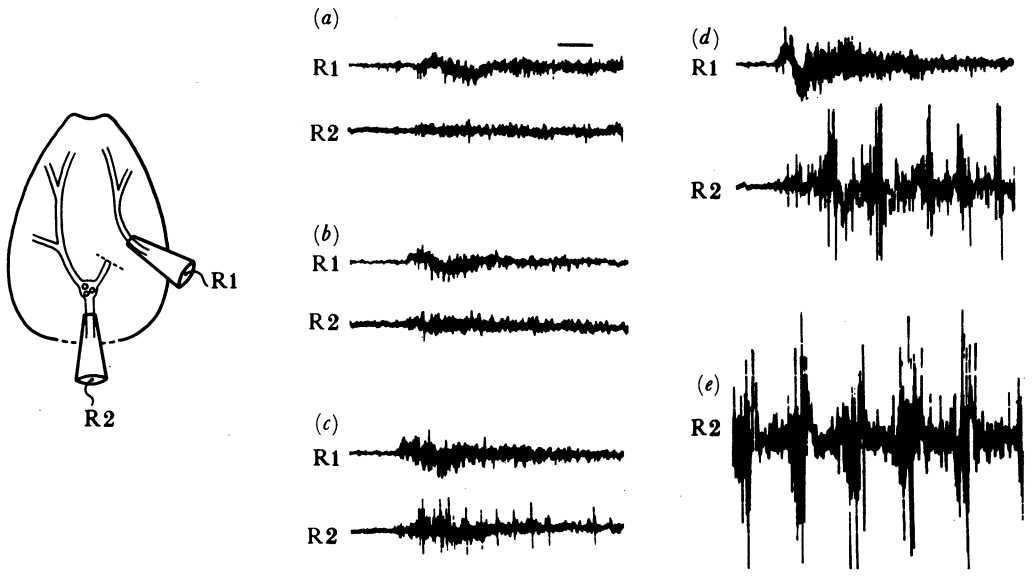

FIGURE 25. Simultaneous responses of a distal nerve and the ceratal nerve, recorded by R1 and R2 as shown on the diagram, during four types of stimulus to the ceras: (*a*) touch by a glass probe; (*b*) touch by a *Pisaster* tube foot; (*c*) first touch by a *Pycnopodia* tube foot; (*d*) second touch by a *Pycnopodia* tube foot; (*e*) pinch by forceps, distal nerve response not shown. Timescale 200 ms.

foot of *Pisaster*. The response of the ceratal nerve was also non-patterned during touches by the glass probe, the tube foot of *Pisaster*, and one of the trials with a *Pycnopodia* tube foot. However, the second application of a *Pycnopodia* tube foot and the pinch produced a dramatic response from the ceratal nerve consisting of repeated bursts of high amplitude, compound spikes (often greater than 200 μV) (figure 25*d*, *e*). The spike bursts were superimposed on a background of non-patterned, low-amplitude neural activity. Once the bursting sequence was initiated within the ceratal nerve, it greatly outlasted the neural activity recorded from the distal nerve. Strong pinches always elicited the patterned output but touches by the *Pycnopodia* tube foot released the pattern in only 35 % of the trials. Furthermore, the mean burst frequency and duration of the patterned output following touch by the *Pycnopodia* tube foot were significantly less than those following a pinch or cut to the ceras (table 1).

The patterned output recorded from the ceratal nerve can also be initiated by a single electrical stimulus to a distal nerve entering a ceratal ganglion. However, activation required that the electrical stimulus surpassed a precise, critical threshold (figure 26). Each preparation required a resting period of 1–2 min before a subsequent electrical stimulus of equal voltage and duration could elicit a renewed discharge of spike bursts.

A subsequent series of experiments showed that the train of spike bursts is carried not only by the ceratal nerve, but also by all distal nerves emerging from primary and secondary ceratal ganglia. Furthermore, the response can be initiated by stimuli to the ceratal nerve. Representative results shown in figure 27*a*, *b* were obtained by dual extracellular recordings from the ceratal nerve and a distal nerve during a single electrical stimulus delivered via a suction electrode to a second distal nerve. Once initiated, the spike bursts occurred synchronously in the distal and ceratal nerves and in no instance was there a difference in the stimulus threshold for eliciting the bursting discharge within any two nerves. Synchronous

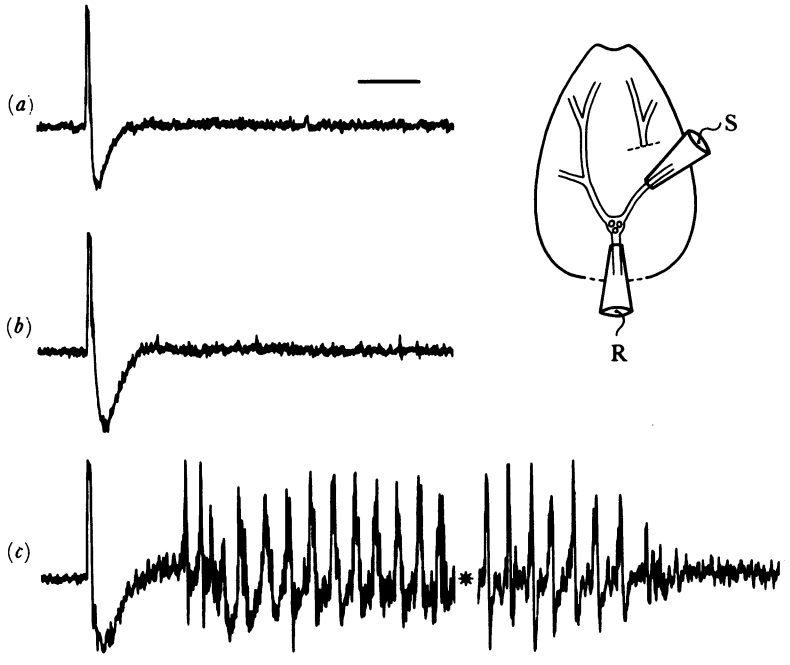

FIGURE 26. Critical stimulus threshold for activation of patterned output. Responses of ceratal nerve, recorded by R as shown on the diagram, following electrical stimulation via S to a distal nerve. Magnitude of stimuli were: (*a*) 6 V, 1.5 ms; (*b*) 8 V, 1.5 ms; (*c*) 10 V, 1.5 ms; the asterisk marks a time gap of 8 s. Timescale 500 ms.

spike bursting in nerves emerging from the ceratal ganglia also occurred when a *Pycnopodia* tube foot provided a suprathreshold stimulus (figure 27*c*).

When preparations like that shown in figures 26 and 27 were bathed for 10 h in artificial seawater containing excess Mg^{2+} and reduced Ca^{2+} to block chemical synapses, the patterned output could still be evoked by electrical stimulation of an emergent nerve.

Finally, experiments in which the connective(s) between primary and secondary ganglia was cut indicated that secondary ganglia, as well as the primary ganglion, can generate the patterned output (figure 28).

Primary ceratal ganglion: intracellular recordings. The patterning and long duration of the signal carried by nerves emerging from ceratal ganglia, compared with the absence of patterning and relatively short duration of signals entering the ganglia following a suprathreshold stimulus, argues that neurons producing the train of spike bursts are postsynaptic to afferent input to the ceratal ganglia. Intracellular recordings from the primary ceratal ganglion indicated that the spike bursts originate from cells located within these peripheral ganglia.

A stimulating suction electrode was applied to an emergent nerve of an isolated primary ceratal ganglion, and a recording suction electrode was applied to a second nerve. After a suprathreshold electrical stimulus, ganglion cells were found that commenced and terminated firing simultaneously with the train of spike bursts recorded extracellularly (figure 29*a*) and each action potential occurred synchronously with each extracellular spike burst (figure 29*b*). Occasionally, during the initial period of spiking, two action potentials occurred during a single extracellular burst. Prepotentials and excitatory postsynaptic potentials (EPSPs) accompanied the action potentials of these cells, which I call synchronous response (SR) neurons. SR neurons

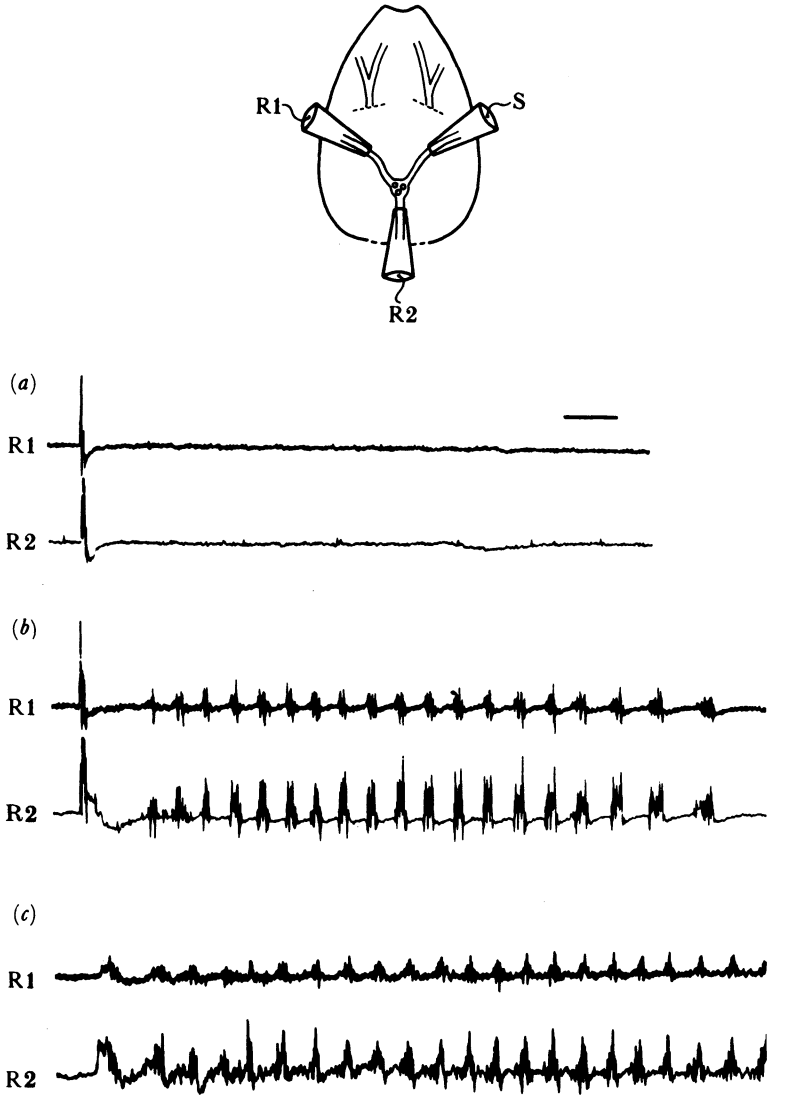

FIGURE 27. Synchrony of spike bursts as recorded from two nerves emerging from the primary ceratal ganglion. The diagram shows positions of recording electrodes, R1 and R2, on a distal nerve and the ceratal nerve, respectively. A second distal nerve was attached to a stimulating electrode, S. (*a*) Electrical stimulus of 8 V, 2 ms; (*b*) electrical stimulus of 10 V, 2 ms; (*c*) *Pycnopodia* tube foot touched to ceratal epidermis (recorded from different preparation to (*a*) and (*b*)). Timescale 500 ms.

remained silent following electrical stimuli that failed to generate a train of spike bursts within the recorded nerve.

Another class of ganglion cells remained silent following a subthreshold stimulus but began spiking soon after a suprathreshold stimulus, yet their action potentials were not synchronous with the extracellular spike bursts and they stopped firing before the end of the extracellular train of bursts (figure 29*c*). A single cell was found that was silent during the train of extracellular spike bursts but showed either a short train of action potentials or a compound EPSP 3–4 s after the end of the extracellular train of bursts. Finally, some cells failed to respond to all electrical stimuli but showed action potentials during intracellular injection of current.

Whole-animal preparation. Whole, unanaesthetized specimens of *M. leonina* were pinned to a

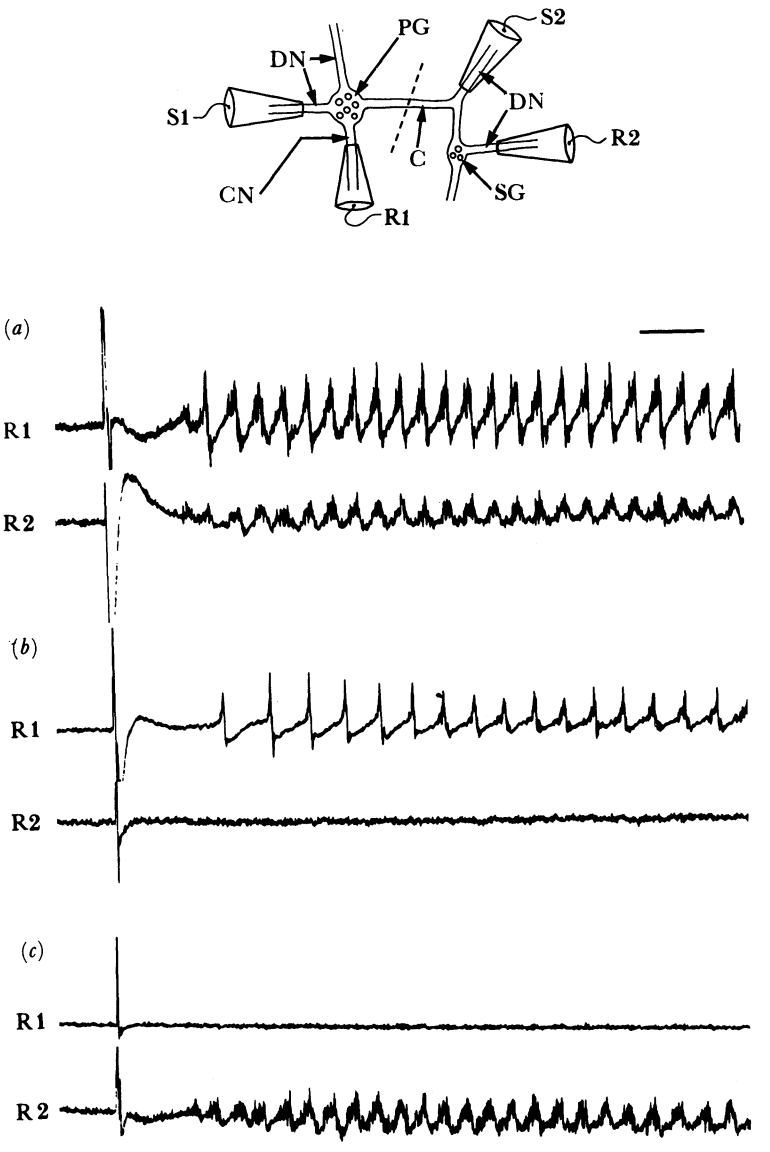

FIGURE 28. Primary and secondary ceratal ganglia can generate patterned output. Diagram shows layout of nerves and ganglia in this preparation. Connective (C), ceratal nerve (CN), distal nerve (DN), primary ceratal ganglion (PG), secondary ceratal ganglion (SG). Records from the ceratal nerve (R1) and a distal nerve arising from the secondary ganglion (R2) during the following manipulations: (*a*) 6.5 V, 2 ms stimulus via S1, connective intact; (*b*) 6.5 V, 2 ms stimulus via S1, connective cut; (*c*) 10 V, 2 ms stimulus via S2 connective cut. Timescale 500 ms.

Sylgard-lined dish and the central ganglia completely removed by an incision through the epidermis behind the oral hood. One ceras was pinned sparingly to the Sylgard and two distal nerves were exposed by a shallow incision made distal to the autotomy plane. One of these distal nerves was cut quickly and cleanly and its proximal end attached to a recording suction electrode (the R nerve; see diagram accompanying figure 30). Many cerata autotomized before electrophysiological recordings could begin, but I was able to obtain extracellular recordings from a distal nerve during the act of ceratal autotomy in 12 preparations. Nevertheless, surgical trauma resulted in obvious constriction of the sphincter muscles flanking

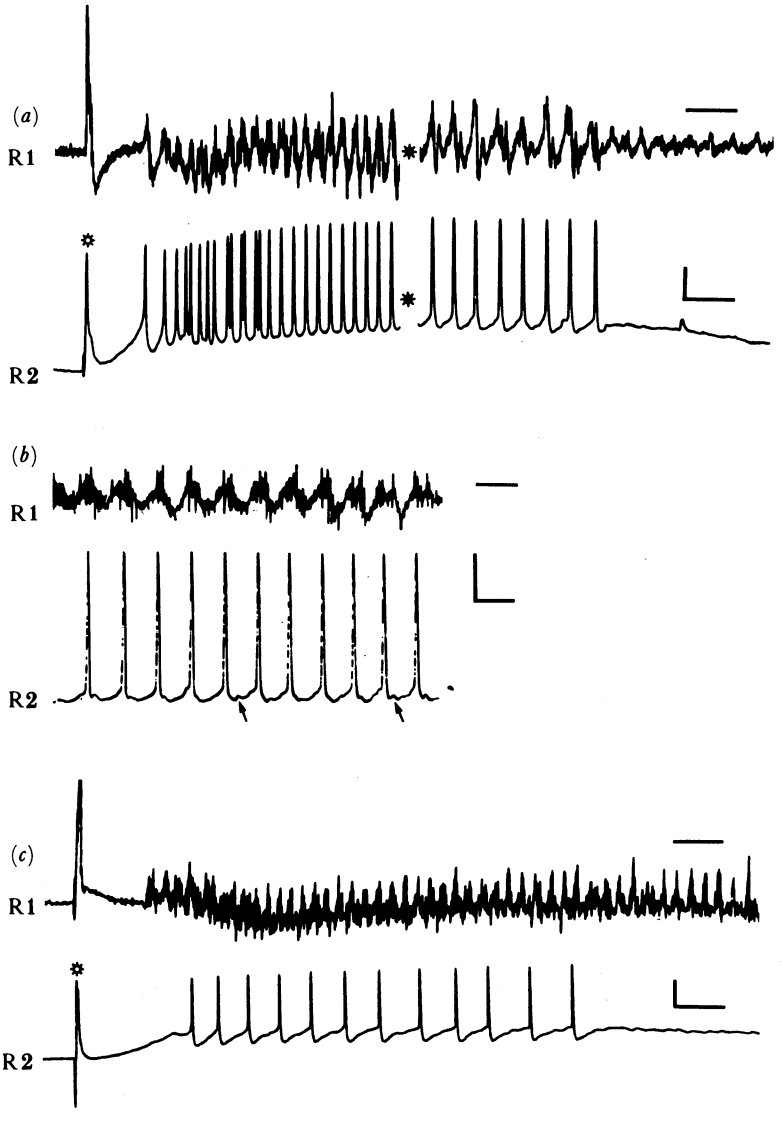

FIGURE 29. Intracellular records (R2) from primary ceratal ganglion neurons and simultaneous extracellular records (R1) from the ceratal nerve following electrical stimulation of a distal nerve. (*a*) SR neuron; antidromic spike (open asterisk) followed by a series of action potentials that begins and ends simultaneously with the extracellular train of spike bursts. Filled asterisks mark time gaps of 10 s. Timescale for R1 and R2 = 100 ms; vertical scale for R2 = 20 mV. (*b*) SR neuron; oscilloscope sweep during recording shown in (*a*). Note synchrony between each intracellular action potential and each spike burst recorded from the ceratal nerve. Also note EPSPs (arrows) preceding action potentials. Timescale for R1 and R2 = 100 ms; vertical scale for R2 = 20 mV. (*c*) Non-SR neuron; antidromic spike (open asterisk) followed by a series of action potentials not coincident with spike bursts recorded from the ceratal nerve. Timescale for R1 and R2 = 300 ms; vertical scale for R2 = 20 mV.

the autotomy plane before the electrode was positioned, suggesting that physiological mechanisms involved in autotomy, though not yet accomplishing actual separation of tissues, were probably begun before the onset of electrophysiological recordings.

At the outset of each experiment, I cut the second distal nerve previously exposed by dissection (the S nerve) while recording from the R nerve. If the cut failed to induce autotomy, the S nerve was attached to a suction stimulating electrode and given electrical stimuli of

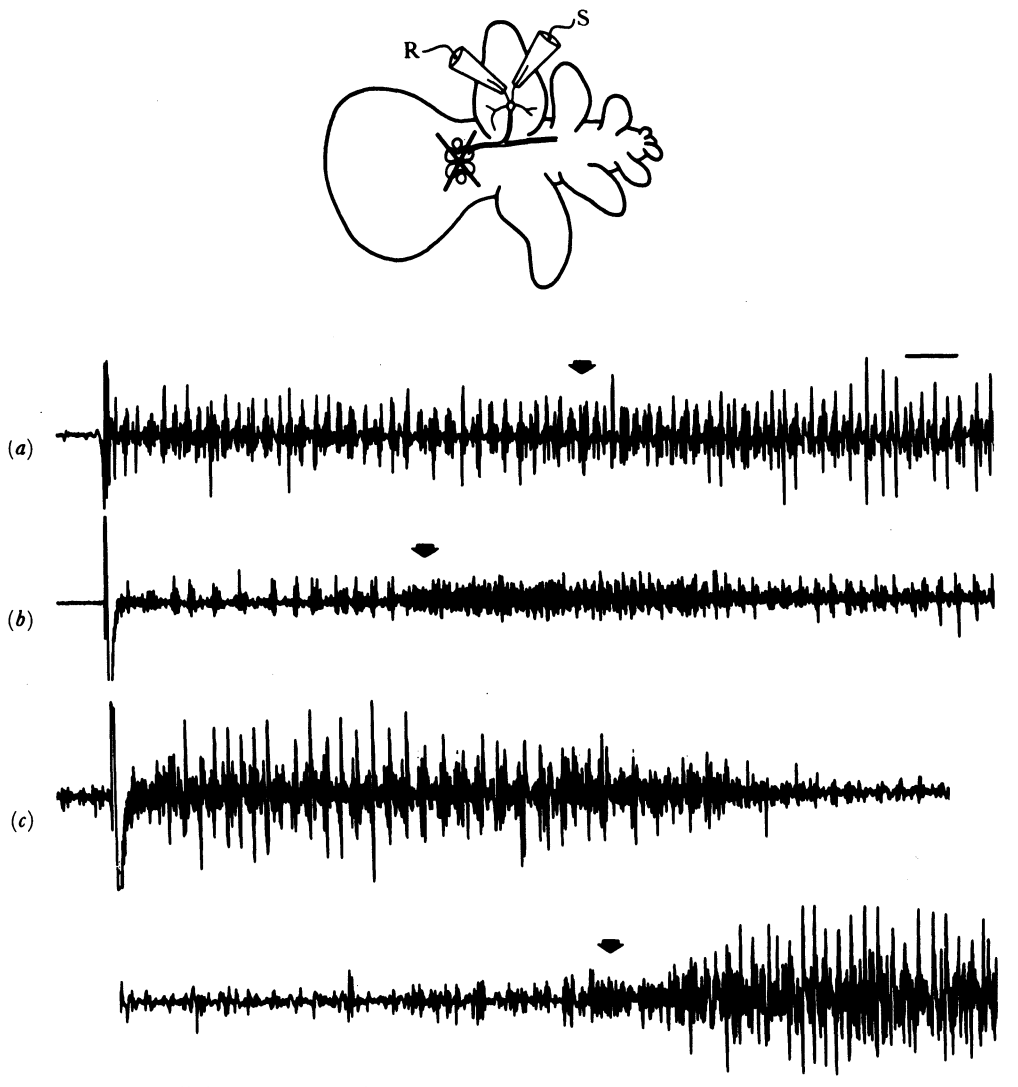

FIGURE 30. Extracellular recordings from a distal nerve (R in the diagram) during ceratal autotomy in three different preparations. CNS removed before each experiment, (*a*) Severing a distal nerve within the ceras induced a train of spike bursts and autotomy of the ceras (arrow) as determined by visual inspection. (*b*) Electrical stimulus to a distal nerve (S on the diagram) induced a train of spike bursts and ceratal autotomy (arrow). Note the 3 s barrage of non-patterned, high-frequency impulses that begins at the onset of autotomy. (*c*) Electrical stimulus to the distal nerve induced a train of spike bursts that arrested 7 s before the onset of ceratal autotomy (arrow). Timescale 500 ms.

progressively greater voltage until autotomy occurred. As shown in figure 30, autotomy was preceded by a sequence of large amplitude, compound-spike bursts within the R nerve that were initiated by cutting or electrically stimulating the S nerve. The train of spike bursts continued after autotomy occurred and in 7 of the 12 preparations, the train of spike bursts was obscured at the time of autotomy and shortly after by a barrage of additional neural discharges (figure 30*b*). The barrage likely represents injury discharges of neurons having axons in both the R nerve and in the ceratal nerve, because the latter is pulled apart as the ceras autotomizes. Previous results showed that an electrical stimulus to the ceratal nerve could generate the patterned output. Therefore rupture and consequent injury discharges of the ceratal nerve

TABLE 1. PARAMETERS OF THE PATTERNED DISCHARGE FOLLOWING FOUR TYPES OF STIMULUS (A–D)

(Bracketed figures following means are range values. Data for A and B were obtained from the ceratal nerve in isolated cerata; data for C and D were obtained from a distal nerve in whole-animal preparations with CNS removed. The means for inter-burst frequency of the patterned output in A and C are both significantly less than the means for interburst frequency in B and D ($p < 0.5$; Student's t-test for unequal sample sizes).)

		parameters of patterned discharge	
stimulus	sample size	mean inter-burst frequency/Hz	mean duration/s
A. *Pycnopodia* tube foot	9	5.1 (3–8)	9.0 (4–15)
B. pinch ceras	12	6.8 (5–11)	21.0 (7–43)
C. non-autotomizing stimulus	11	5.3 (3–9)	4.5 (3–6)
D. autotomizing stimulus	12	7.9 (5–14)	9.8 (2–30)

would explain why the patterned output is renewed, often with increased burst frequency and for long duration, immediately after autotomy takes place.

Figure 30*c* shows a short quiescent period between the end of a patterned output within the R nerve and the occurrence of autotomy. Injury spiking and a renewal of the patterned output were initiated at the time of autotomy. This was found in 2 of the 12 preparations and a possible interpretation is given in the Discussion.

Stimuli to the S nerve that activated the patterned output within the R nerve did not always result in autotomy in whole-animal preparations. Nevertheless, patterned outputs were accompanied by abrupt twitches of the sphincter muscles and longitudinal muscle bands. The train of spike bursts following non-autotomizing stimuli showed a significantly lower burst frequency and a shorter train duration than the trains of spike bursts resulting in autotomy (table 1).

DISCUSSION

(*a*) *Mechanism of autotomy*

My observations of ceratal autotomy by live *M. leonina* and, particularly, of the ultrastructure of the autotomy plane before and after separation suggest that granule-filled cells (GCs) and muscle contraction participate in the autotomy mechanism.

(i) *Granule-filled cells (GCs)*

The distribution of GCs, their degranulation during autotomy, and their apparent innervation by axons extending from within the ceras strongly imply a role in the autotomy mechanism of cerata. At present, I can only speculate on this role. Nevertheless, existing evidence shows notable structural similarities between the ceratal autotomy plane of *M. leonina* and autotomy planes of several echinoderms, for which the autotomy mechanism is better understood.

Rapid, irreversible loss of tensile strength by interstitial and basal lamina-derived collagenous structures is the underlying mechanism of autotomy in echinoderms, as determined for an ophiuroid (see Wilkie 1978*a*, *b*, 1979; Wilkie & Emson 1987), a crinoid (see Holland & Grimmer 1981), and a holothuroid (see Byrne 1985*a*, *b*, 1986). The phenomenon is an extreme and irreversible expression of a more widespread ability by many echinoderm collagenous structures to switch rapidly, yet reversibly, between extensible and inextensible ('catch') states

(see reviews by Emson & Wilkie (1980); Wilkie (1984); Motokawa (1984)). The excellent work of Hidaka & Takahashi (1983) on the catch apparatus of echinoid spines has shown that collagen fibrils can slide past one another during the extensible state, but become locked in place during the catch state. Furthermore, the mechanical properties of *in vitro* preparations of echinoderm connective tissues of variable tensile strength are sensitive to pH, ionic strength, divalent cation concentration (particularly Ca^{2+}) and calcium ion chelators (see Wilkie 1978*b*, 1983; Smith *et al.* 1981; Eylers 1982; Hidaka 1983; Byrne 1985*b*). These results suggest that the collagen fibrils may be interlinked by non-covalent interactions (particularly electrostatic bonds) with and between proteoglycans or glycoproteins of the extracellular matrix, which may be altered by active control of local pH or cation concentration (see Wilkie 1984; Motokawa 1984).

Cytoplasmic processes of innervated neurosecretory-like cells ('juxtaligamental cells' described by Wilkie (1979)) containing large, spherical or ovoid, membrane-bounded granules are a consistent feature of echinoderm connective tissues of variable tensile strength (see Wilkie 1984). Several studies have reported degranulation of these cells at sites of collagenous tissue rupture during echinoderm autotomy (Holland & Grimmer 1981; Hilgers & Splechtna 1982; Wilkie & Emson 1987).

There are at least four specific similarities between the autotomy planes of echinoderms and the ceratal autotomy plane of *M. leonina*. First, the ceratal autotomy plane is not inherently fragile, despite the basal narrowing of cerata. This is also true of the autotomy planes of echinoderms, as first emphasized by Wilkie (1978*a*) for ophiuroid arms. Second, in *M. leonina* and in echinoderms, cytoplasmic processes containing many electron-dense granules are associated with connective tissue structures that rupture during autotomy. Third, the GCs of *M. leonina* and the granular cells associated with autotomizing structures in echinoderms are innervated. Finally, preliminary evidence suggests that, like the autotomizing structures of echinoderms, tissue breakage at the ceratal autotomy plane of *M. leonina* may be facilitated by some type of disruption of connective-tissue components. Deprived of these strengthening elements, epithelial, muscular and nervous tissue should be susceptible to mechanical failure under tensile stress. Indeed, close inspection of the process of epidermal separation along the ceratal autotomy plane of *M. leonina* recalls Stasek's (1967) translation of Quoy & Gaimard's (1832) description of pedal autotomy in the prosobranch *Harpa ventricosa*: '...the separation resembling an ungluing rather than a tearing of tissues'.

Before further comparisons can be made between echinoderm autotomy and ceratal autotomy in *M. leonina*, additional work is needed to confirm the collagenous nature of basal lamina and interstitial connective tissue within the ceratal autotomy plane, to examine in greater detail the fate of this connective tissue during autotomy, to determine the mechanical properties of the connective tissue under conditions of different pH, ionic strength and cation composition, and to examine the chemical composition of the granular product of GCs.

Comparative studies are needed to determine if GCs are present within the autotomy planes of other molluscs. It is intriguing that Kress (1968), using light microscopy, identified a granular zone at the base of the deciduous cerata of three species of *Doto* (Nudibranchia), although the GC granules of *M. leonina* are not resolvable in 1 μm sections. In the only other ultrastructural study of the autotomy plane of a mollusc, Hodgson (1984) concluded that siphonal autotomy in two species of *Solen* (Bivalvia) is the result of muscle contraction and zones of weakness (reduced connective tissue) within the wall of the siphon. He did not describe GCs within the potential autotomy sites.

(ii) *Muscles*

Although GCs may provide the major mechanism for ceratal autotomy in *M. leonina*, ceratal muscles must play a contributory role. Strong contractions of the sphincter muscles and, less obviously, the longitudinal muscle bands precede and accompany ceratal autotomy.

The longitudinal muscle bands are composed of a staggered array of parallel muscle cells invested with connective tissue fibrils and hemifasciae adherentes are common along the sarcolemmae. Twarog *et al.* (1973) and Nunzi & Franzini-Armstrong (1981) suggest that hemifasciae adherentes in molluscan muscle link intracellular and extracellular fibrillar elements and may allow some of the very large tension generated by these muscles to be safely transferred to connective tissue components. Normally, the connective tissue binding each longitudinal muscle band must be sufficiently strong to withstand the tensile stress experienced during contraction of the component muscle cells, resulting in a shortening of the entire muscle band. However, if this connective tissue suddenly lost tensile strength where the longitudinal muscle bands cross the autotomy plane (possibly by the action of GC granules), contraction would result in disjunction of the muscle band at the site of the weakened connective tissue.

On either side of the autotomy plane, the longitudinal muscle bands are attached to the epidermis via the two sphincter muscles. Consequently, once the longitudinal muscle bands have broken, tensile stress must be transmitted to the epidermis at the level of the autotomy plane. Cytoplasmic extensions from the GCs are associated with the epidermis at the level where this stress would be experienced.

At least three functions can be envisaged for contraction of the sphincter muscles during autotomy. First, sphincter contraction may prevent fluid from leaving the ceras during contraction of the longitudinal muscle bands. This would provide the ceras with a rigid hydraulic skeleton, allowing the contracting longitudinal muscle bands on the ceratal side of the autotomy plane to generate the large tensile stresses that help to separate tissues. Second, subepidermal sphincter contraction may assist in breaking the longitudinal muscle bands by exerting an additional stress, directed at right angles to that generated by contraction of the muscle band itself, on the autotomy planes of these muscles. Finally as previously suggested by Graham (1938) for the ceratal sphincter muscles of several aeolids, sphincter contraction closes the wound resulting from ceratal autotomy.

(*b*) *Neural correlate of autotomy*

Extracellular recordings from all nerves leaving ceratal ganglia show a distinctive signal, consisting of repeated bursts of large amplitude, compound spikes, following strong aversive stimuli (cuts or strong pinches) to the ceratal epidermis or a suprathreshold electrical stimulus to a nerve entering a ceratal ganglion. In whole *M. leonina*, strong aversive stimuli to a ceras are both necessary and sufficient to cause autotomy of that ceras and the distinctive extracellular signal precedes autotomy. Collectively, these results suggest that the train of spike bursts generated by ceratal ganglia is involved in signalling autotomy behaviour.

Intracellular recordings from the primary ceratal ganglion identified so-called SR neurons that commence and terminate firing simultaneously with the patterned output recorded extracellularly from a nerve leaving the ganglion, and each action potential (rarely two) occurs simultaneously with each extracellular spike burst. These cells also show an antidromic spike following electrical stimuli to a distal nerve entering the ganglion. No cells were found that showed bursts of action potentials. Therefore I suggest that the extracellular train of spike

bursts results from a network of SR neurons, which are coordinated to fire in synchrony and which collectively send at least several axons into each nerve leaving the ganglion. Results of the experiment shown in figure 28 indicate that a network of SR neurons resides in primary and secondary ceratal ganglia and the activity of each network is synchronized with that of other ganglia.

The most likely explanation for synchronous activity of SR neurons is electrical coupling between them. This explanation is consistent with two other observations. First, high Mg^{2+}, low Ca^{2+} artificial seawater failed to block the train of spike bursts elicited by an electrical stimulus to a distal nerve. This result also shows that SR neurons send axons into nerves extending from ceratal ganglia (for antidromic conduction along SR axons within the stimulated nerve and orthodromic conduction along SR axons within the recorded nerve). Second, the train of spike bursts requires high stimulus intensity for activation. Populations of electrically coupled neurons have low input resistances due to shunting of current throughout the group; these cells require large synaptic currents for depolarization. Carew & Kandel (1977) suggested that electrical coupling among motorneurons innervating the ink gland of *Aplysia californica* is part of the reason for the strong stimulus requirement for activation of these motorneurons.

Three potential targets, either directly or indirectly, for SR neurons are the repugnatorial glands, the GCs associated with the nerve rings within the autotomy plane, and the ceratal muscles. As described by Page (1988), the secretory cells and muscles of repugnatorial glands receive chemical synapses and a bundle of axons is associated with each gland. However, direct touch to the epidermis overlying each gland was the only stimulus that discharged the glands, and glandular discharge was never observed coincident with the train of spike bursts. The highly localized stimulus–response character of repugnatorial-gland discharge and the finding that the train of spike bursts, once initiated, is carried by all nerves emerging from ceratal ganglia is inconsistent with the notion that repugnatorial glands are the target of SR neurons. Many axons within the nerve bundle associated with each repugnatorial gland are probably afferent fibres originating from ciliated receptor cells adjacent to the pore of each gland. The possibility remains that the SR neurons act on repugnatorial glands to alter their threshold for discharge.

Although the GCs within the autotomy plane may be an indirect or a partial target for SR neurons (see further discussion below), the fact that the patterned output is carried by all nerves emerging from ceratal ganglia argues against the possibility that GCs are the exclusive target for this signal. In young juveniles at least, the ceratal nerve is the exclusive source of axons extending to the autotomy plane nerve rings where innervated GCs are located.

The longitudinal muscle bands of the ceras are each composed of many muscle cells that collectively extend from the apex of the ceras into its base and continue into the body proper. Unquantified observations showing contraction of the longitudinal muscle bands and the basal sphincter muscles coincident with the patterned output, and the fact that the patterned output is carried by nerves extending from ceratal ganglia to regions throughout the ceras, suggest that the SR neurons are efferents to the longitudinal and sphincter muscles. This suggestion is consistent with the fact that the patterned output precedes ceratal autotomy, because my model of the autotomy mechanism states that strong contractions of the sphincter and longitudinal muscle bands help separate tissues during ceratal autotomy.

If SR neurons are indeed efferents to ceratal muscles, what might be the functional

importance of their synchronized spiking? During a discussion of the stimulus–response characteristics of several neuromuscular systems in the bivalve *Spisula solidissima*, Prior (1975) noted that efferents to the siphon retractor muscle show non-coincident activity and the muscle exhibits graded contractions. However, motorneurons to the fast shell adductors show highly coincident activity that is correlated with strong, synchronous contractions of the muscle mass. Similarly, the co-occurrence of action potentials among SR neurons may generate strong, synchronous contractions of ceratal muscles.

The hypothesis that coordinated activity of SR neurons is part of the neural effector system for autotomy has a potential problem. Touches by tube feet of *Pycnopodia* to cerata of *M. leonina* never caused ceratal autotomy, yet in isolated cerata 35% of the *Pycnopodia* touches initiated the patterned output from nerves emanating from the basal ganglion. Furthermore, in whole-animal preparations, electrical stimuli of sufficient strength to generate the patterned output were not always sufficient to initiate ceratal autotomy. Two observations may resolve this apparent paradox.

First, the patterned output varied in its duration and burst frequency and these parameters may affect strength of response by targets of SR neurons. As shown in table 1, significant differences in both these parameters of the patterned output were found for *Pycnopodia* touches compared with pinches or cuts to the cerata epidermis in isolated cerata, and for autotomizing compared with non-autotomizing stimuli in whole-animal preparations. Many, although not all, studies on molluscan muscle have found that muscle tension is proportional to the size of the junction potential and the latter often responds to the duration and temporal pattern of arriving impulses by showing summation, facilitation and post-tetanic potentiation (Carew *et al.* 1974; Blankenship *et al.* 1977; Rock *et al.* 1977; Cohen *et al.* 1978; Peters & Altrup 1984).

The requirement for degranulation of GCs during ceratal autotomy is the second, and probably more important, reason why some discharges of SR neurons are insufficient to release autotomy behaviour. Because autotomy is a drastic all-or-none behaviour to be employed only in extremely threatening situations, the neurons innervating GCs, or GCs themselves, must have a very high threshold for activation. Presumably, strong mechanical insults are capable of surpassing their threshold, whereas *Pycnopodia* tube foot touches are not. One attractive possibility is that SR neurons innervate GCs, as well as ceratal muscles, but the spike frequency and possibly train duration of SR neurons must surpass a critical threshold before GCs are activated to release their granules. Future studies will investigate this possibility.

The foregoing observations lead me to propose that synchronous contractions of ceratal muscles, as directed by SR neurons may be part of a general body contraction response to noxious (*Pycnopodia* tube foot) or strong mechanical stimuli to a ceras. However, only when the muscle contractions are sufficiently strong, and particularly, only when they are coupled to GC degranulation, does autotomy behaviour ensue.

The short quiescent period between the end of the patterned output and the onset of ceratal autotomy seen in two of the whole-animal preparations (figure 30*c*) may represent a time period necessary for exocytosed GC granules to disrupt connective-tissue structures within the autotomy plane.

In conclusion, my observations suggest that at least some peripheral neurons contained within cerata of *M. leonina* are efferents, probably to ceratal muscles. In this regard, they are similar to peripheral neurons within the siphon of *Aplysia californica* (Bailey *et al.* 1979) and the siphons of *Spisula solidissima* (Prior 1972*a*, *b*). However, whereas peripheral effectors within the

siphons of *Spisula* mediate small local contractions to weak stimuli and those within the siphon of *Aplysia* cooperate with central motorneurons to effect siphon withdrawal, peripheral effectors in cerata of *M. leonina* may be entirely responsible for a dramatic defensive behaviour: autotomy of the ceras. This working hypothesis requires further experimentation, particularly regarding the location of neurons innervating GCs and confirmation that SR neurons innervate ceratal muscles.

Thanks to C. Pennachetti, I. Boyd and Dr M. Byrne for collecting specimens, and to Dr A. O. D. Willows and his staff at Friday Harbor Laboratories, University of Washington, U.S.A. Dr A. R. Fontaine, Dr D. H. Paul, Dr D. J. Prior and Dr I. C. Wilkie gave helpful comments on an earlier draft of this manuscript. I am particularly grateful to Dr G. O. Mackie for technical assistance, valuable discussion and manuscript review. This work was supported by NSERC research grant to G. O. Mackie and a University of Victoria Postgraduate Fellowship.

References

Agersborg, H. P. 1921 Contribution to the knowledge of the nudibranchiate mollusk, *Melibe leonina* (Gould). *Am. Nat.* **55**, 222–253.

Agersborg, H. P. 1923 A critique on professor Harold Heath's *Chioraera dalli*, with special reference to the use of the foot in the nudibranchiate mollusk, *Melibe leonina* Gould. *Nautilus* **36**, 86–96.

Ajeska, R. A. & Nybakken, J. 1976 Contributions to the biology of *Melibe leonina* (Gould, 1852). *Veliger* **19**, 19–26.

Audesirk, G. & Audesirk, T. 1980 Complex mechanoreceptors in *Tritonia diomedea*. I. Responses to mechanical and chemical stimuli. *J. comp. Physiol.* A **141**, 101–109.

Bailey, C. H., Castellucci, V. F., Koester, J. & Kandel, E. R. 1979 Cellular studies of peripheral neurons in siphon skin of *Aplysia californica*. *J. Neurophysiol.* **42**, 530–557.

Bickell, L. R. & Kempf, S. C. 1983 Larval and metamorphic morphogenesis in the nudibranch *Melibe leonina* (Mollusca: Opisthobranchia). *Biol. Bull. mar. biol. Lab., Woods Hole* **165**, 119–138.

Blankenship, J. E., Rock, M. K. & Hill, J. 1977 Physiological properties of the penis retractor muscle of *Aplysia*. *J. Neurobiol.* **8**, 549–568.

Byrne, M. 1985*a* Ultrastructural changes in the autotomy tissues of *Eupentacta quinquesemita* (Selenka) (Echinodermata: Holothuroidea) during evisceration. In *Proceedings of the Fifth International Echinoderm Conference, Galway* (ed. B. F. Keegan & B. D. S. O'Connor), pp. 413–420. Rotterdam: A. A. Balkema.

Byrne, M. 1985*b* The mechanical properties of the autotomy tissues of the holothurian *Eupentacta quinquesemita* and the effects of certain physico-chemical agents. *J. exp. Biol.* **117**, 69–86.

Byrne, M. 1986 Induction of evisceration in the holothurian *Eupentacta quinquesemita* and evidence for the existence of an endogenous evisceration factor. *J. exp. Biol.* **120**, 25–39.

Carew, T. J. & Kandel, E. R. 1977 Inking in *Aplysia californica*. I. Neural circuit of an all-or-none behavioral response. *J. Neurophysiol.* **40**, 692–707.

Carew, T. J., Pinsker, H., Rubinson, K. & Kandel, E. R. 1974 Physiological and biochemical properties of neuromuscular transmission between identified motoneurons and gill muscle in *Aplysia*. *J. Neurophysiol.* **37**, 1020–1040.

Cloney, R. A. & Florey, E. 1968 Ultrastructure of cephalopod chromatophore organs. *Z. Zellforsch. mikrosk. Anat.* **89**, 73–79.

Cohen, J. L., Weiss, K. R. & Kupfermann, I. 1978 Motor control of buccal muscles in *Aplysia*. *J. Neurophysiol.* **41**, 157–180.

Congdon, J. D., Vitt, L. J. & King, W. W. 1974 Geckos: adaptive significance and energetics of tail autotomy. *Science, Wash.* **184**, 1370–1380.

Dial, B. E. & Fitzpatrick, L. C. 1983 Lizard tail autotomy: function and energetics of postautotomy tail movement in *Scincella lateralis*. *Science, Wash.* **219**, 391–393.

Emson, R. H. & Wilkie, I. C. 1980 Fission and autotomy in echinoderms. *Oceanogr. mar. Biol.* **18**, 155–250.

Eylers, J. P. 1982 Ion-dependent viscosity of holothurian body wall and its implications for the functional morphology of echinoderms. *J. exp. Biol.* **99**, 1–8.

Frédéricq, L. 1883 Sur l'autotomie ou mutilation par voie réflexe comme moyen de défense chez les animaux. *Archs Zool. exp. gén.* (ser. 2) **1**, 413–426.

Graham, A. 1938 The structure and function of the alimentary canal of aeolid molluscs, with a discussion on their nematocysts. *Trans. R. Soc. Edinb.* **59**, 267–307.

Hidaka, M. 1983 Effects of certain physico-chemical agents on the mechanical properties of the catch apparatus of the sea-urchin spine. *J. exp. Biol.* **103**, 15–29.

Hidaka, M. & Takahashi, T. 1983 Fine structure and mechanical properties of the catch apparatus of the sea-urchin spine, a collagenous connective tissue with muscle-like holding capacity. *J. exp. Biol.* **103**, 1–14.

Hilgers, M. & Splechtna, H. 1982 Zur Steuerung der Ablosung von Giftpedizellarien bei *Sphaerechinus granularis* (Lam.) und *Paracentrotus lividus* (Lam.) (Echinodermata, Echinoidea). *Zool. Jb.* II **107**, 442–457.

Hodgson, A. N. 1984 Use of the intrinsic musculature for siphonal autotomy in the Solenacea (Mollusca: Bivalvia). *Trans. R. Soc. S. Afr.* **45**, 129–138.

Holland, N. D. & Grimmer, J. C. 1981 Fine structure of syzygial articulations before and after arm autotomy in *Florometra serratissima* (Echinodermata: Crinoidea). *Zoomorphologie* **98**, 169–183.

Hurst, A. 1968 The feeding mechanism and behavior pattern of the opisthobranch *Melibe leonina*. *Symp. zool. Soc. Lond.* **22**, 151–166.

Jensen, K. R. 1984 Defensive behavior and toxicity of ascoglossan opisthobranch *Mourgona germaineae* Marcus. *J. chem. Ecol.* **10**, 475–486.

Kandel, E. R. 1976 *Cellular basis of behavior: an introduction to behavioral neurobiology*. San Francisco: W. H. Freeman.

Kandel, E. R. 1979 *Behavioral biology of Aplysia: a contribution to the comparative study of opisthobranch molluscs*. San Francisco: W. H. Freeman.

Kress, A. 1968 Untersuchungen zur Histologie, Autotomie und Regeneration dreier *Doto* – Arten *Doto coronata*, *D. pinnatifida*, *D. fragilis* (Gastropoda, Opisthobranchiata). *Revue suisse Zool.* **75**, 225–303.

Luft, J. H. 1961 Improvements in epoxy resin embedding methods. *J. biophys. biochem. Cytol.* **9**, 409–414.

Lukowiak, K. & Jacklet, J. W. 1972 Habituation and dishabituation: interactions between peripheral and central nervous systems. in *Aplysia*. *Science, Wash.* **178**, 1306–1308.

Lukowiak, K. & Jacklet, J. W. 1975 Habituation and dishabituation mediated by the peripheral and central neural circuits of the siphon of *Aplysia*. *J. Neurobiol.* **6**, 183–200.

Mauzey, K. P., Birkeland, C. & Dayton, P. K. 1968 Feeding behavior of asteroids and escape responses of their prey in the Puget Sound region. *Ecology* **49**, 606–619.

McVean, A. 1974 The nervous control of autotomy in *Carcinus maenas*. *J. exp. Biol.* **60**, 423–436.

McVean, A. 1975 Autotomy. *Comp. Biochem. Physiol.* A **51**, 497–505.

McVean, A. 1982 Autotomy. In *Biology of Crustacea* (ed. D. C. Sandeman & H. L. Atwood), pp. 107–132. New York: Academic Press.

McVean, A. & Findlay, I. 1976 Autotomy in *Carcinus maenas*: the role of the basiischiopodite posterior levator muscles. *J. comp. Physiol.* A **110**, 367–381.

Motokawa, T. 1984 Connective tissue catch in echinoderms. *Biol. Rev.* **59**, 255–270.

Nicaise, G. 1973 The gliointerstitial system of molluscs. *Int. Rev. Cytol.* **34**, 251–332.

Nunzi, M. G. & Franzini-Armstrong, C. 1981 The structure of smooth and striated portions of the adductor muscle of the valves in a scallop. *J. Ultrastruct. Res.* **76**, 134–148.

Page, L. R. 1988 The cerata of *Melibe leonina* (Gould, 1859) (Mollusca; Nudibranchia): morphogenesis, neurogenesis, autotomy, and repugnatorial glands. Ph.D. dissertation, University of Victoria, Victoria, British Columbia.

Peretz, B., Jacklet, J. W. & Lukowiak, K. 1976 Habituation of reflexes in *Aplysia*: contribution of the peripheral and central nervous systems. *Science, Wash.* **191**, 396–399.

Perlman, A. J. 1979 Central and peripheral control of siphon-withdrawal reflex in *Aplysia californica*. *J. Neurophysiol.* **42**, 510–529.

Peters, M. & Altrup, U. 1984 Motor organization in pharynx of *Hélix pomatina*. *J. Neurophysiol.* **52**, 389–409.

Prior, D. J. 1972*a* Electrophysiological analysis of peripheral neurones and their possible role in the local reflexes of a mollusc. *J. exp. Biol.* **57**, 133–145.

Prior, D. J. 1972 *b* A neural correlate of behavioural stimulus intensity discrimination in a mollusc. *J. exp. Biol.* **57**, 147–160.

Prior, D. J. 1975 A study of the electrophysiological properties of the incurrent siphonal valve muscle of the surf clam, *Spisula solidissima*. *Comp. Biochem. Physiol.* A **52**, 607–610.

Quoy, J. R. C. & Gaimard, J. P. 1832 *Voyage de decouvertes de l'Astrolabe. Zoologie, Paris* **2**, 1–686.

Rock, M. K., Blankenship, J. E. & Lebeda, F. J. 1977 Penis-retractor muscle of *Aplysia*: excitatory motor neurons. *J. Neurobiol.* **8**, 569–579.

Sheppard, L. & Bellairs, Ad'A. 1972 The mechanism of autotomy in *Lacerta*. *Br. J. Herpet.* **4**, 276–286.

Smith, C. N. & Greenberg, M. J. 1973 Chemical control of the evisceration process in *Thyone briareus*. *Biol. Bull. mar. biol. Lab., Woods Hole* **144**, 421–436.

Smith, D. S., Wainwright, S. A., Baker, J. & Cayer, M. L. 1981 Structural features associated with movement and 'catch' of sea-urchin spines. *Tiss. Cell.* **13**, 299–320.

Stasek, C. R. 1967 Autotomy in the Mollusca. *Occ. Pap. Calif. Acad. Sci.* **61**, 1–44.

Twarog, B. M., Dewey, M. H. & Hikado, T. 1973 The structure of *Mytilus* smooth muscle and the electrical constants of the resting muscle. *J. gen. Physiol.* **61**, 207–221.

Wake, D. B. & Dresner, I. G. 1967 Functional morphology and evolution of tail autotomy in salamanders. *J. Morph.* **122**, 265–306.

Wilkie, I. C. 1978*a* Functional morphology of the autotomy plane of the brittlestar *Ophiocomina nigra* (Abildgaard) (Ophiuroidea, Echinodermata). *Zoomorphologie* **91**, 289–305.
Wilkie, I. C. 1978*b* Nervously mediated change in the mechanical properties of a brittlestar ligament. *Mar. Behav. Physiol.* **5**, 289–306.
Wilkie, I. C. 1979 The juxtaligamental cells of *Ophiocomina nigra* (Abildgaard) (Echinodermata: Ophiuroidea) and their possible role in mechano-effector function of collagenous tissue. *Cell Tiss. Res.* **197**, 515–530.
Wilkie, I. C. 1983 Nervously mediated change in the mechanical properties of the cirral ligaments of a crinoid. *Mar. Behav. Physiol.* **9**, 229–248.
Wilkie, I. C. 1984 Variable tensility in echinoderm collagenous tissues: a review. *Mar. Behav. Physiol.* **11**, 1–34.
Wilkie, I. C. & Emson, R. H. 1987 The tendons of *Ophiocomina nigra* and their role in autotomy (Echinodermata, Ophiuroidea). *Zoomorphology* **107**, 33–44.

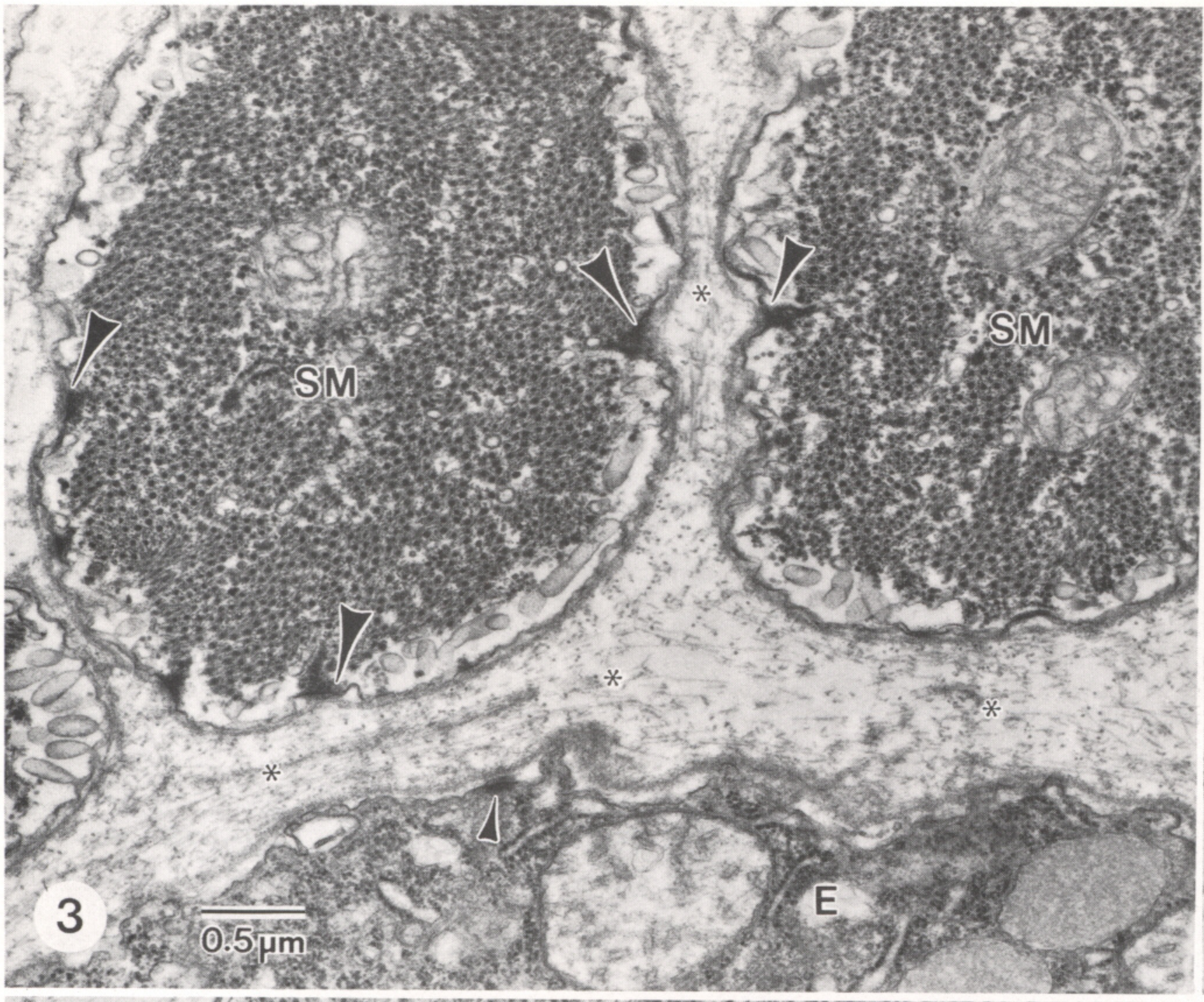

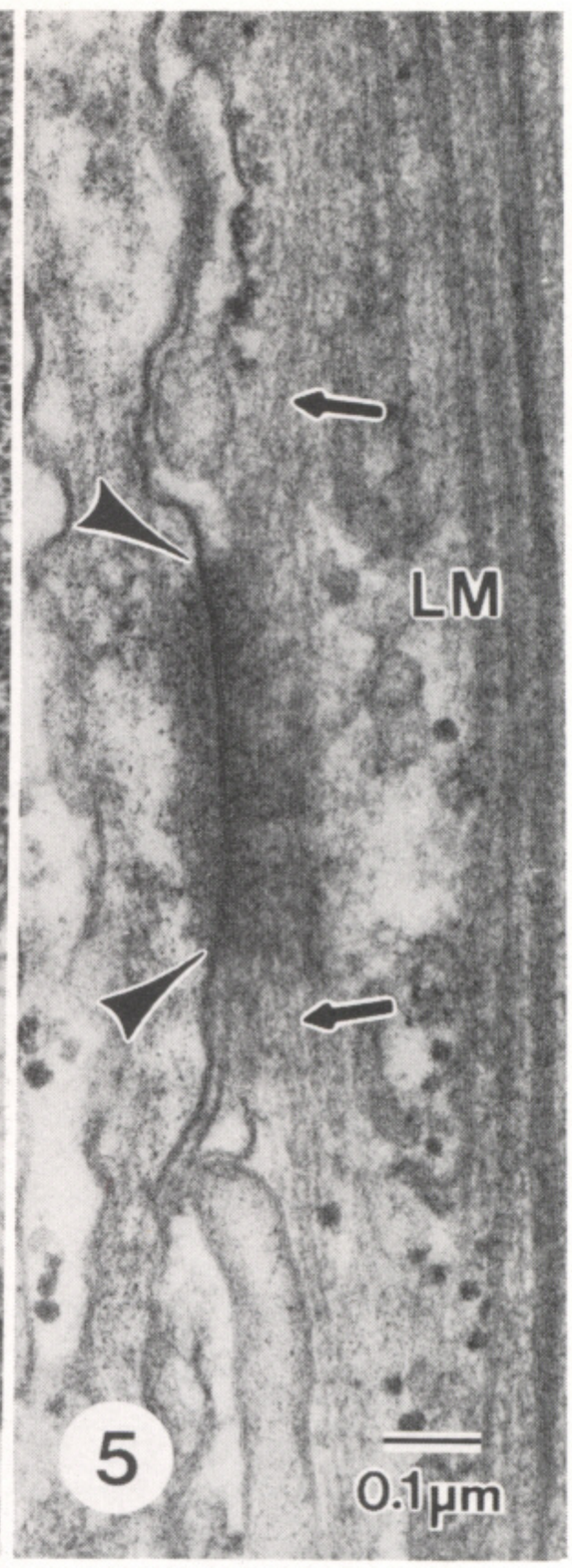

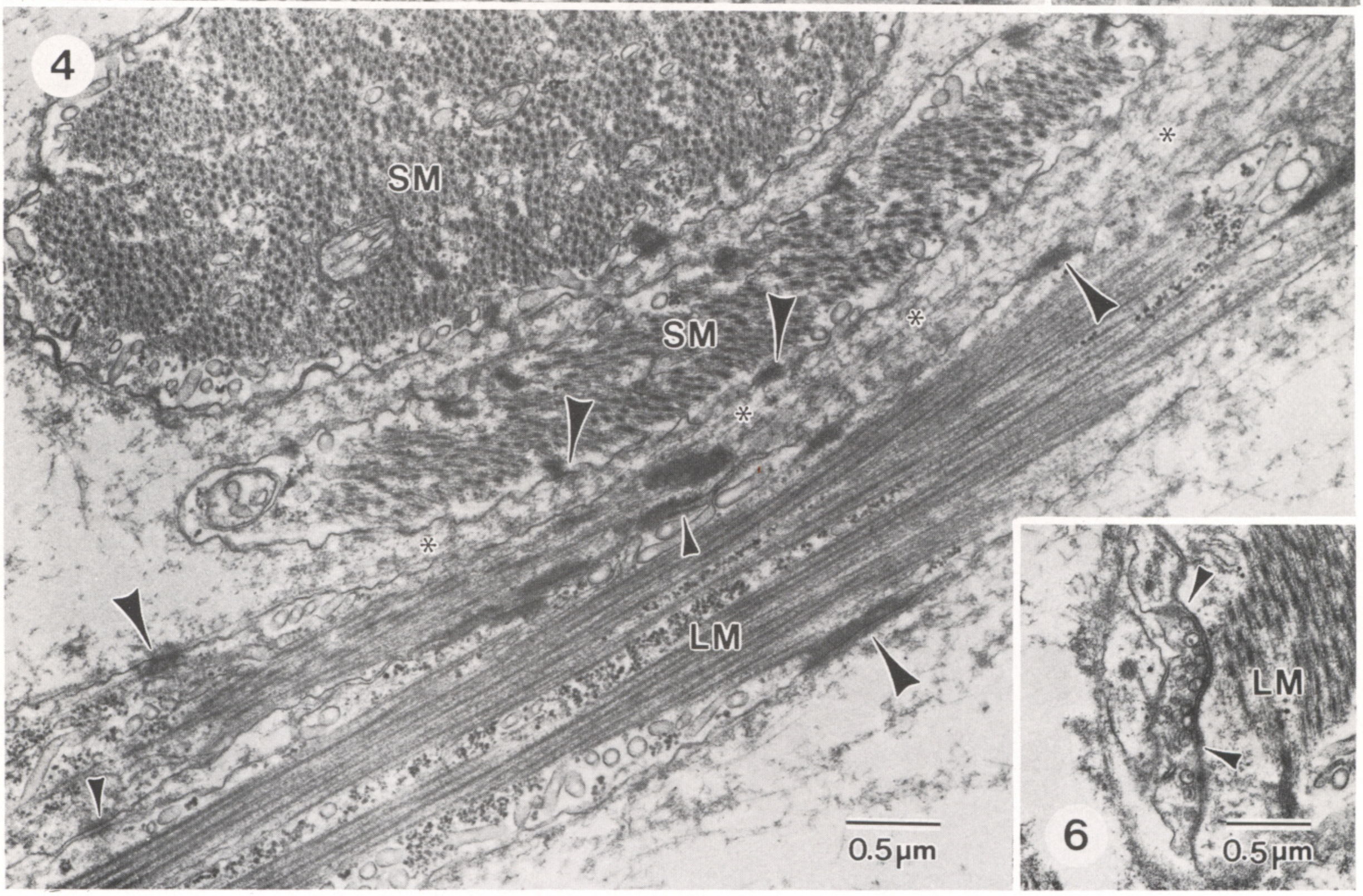

FIGURES 3–6. For description see opposite.

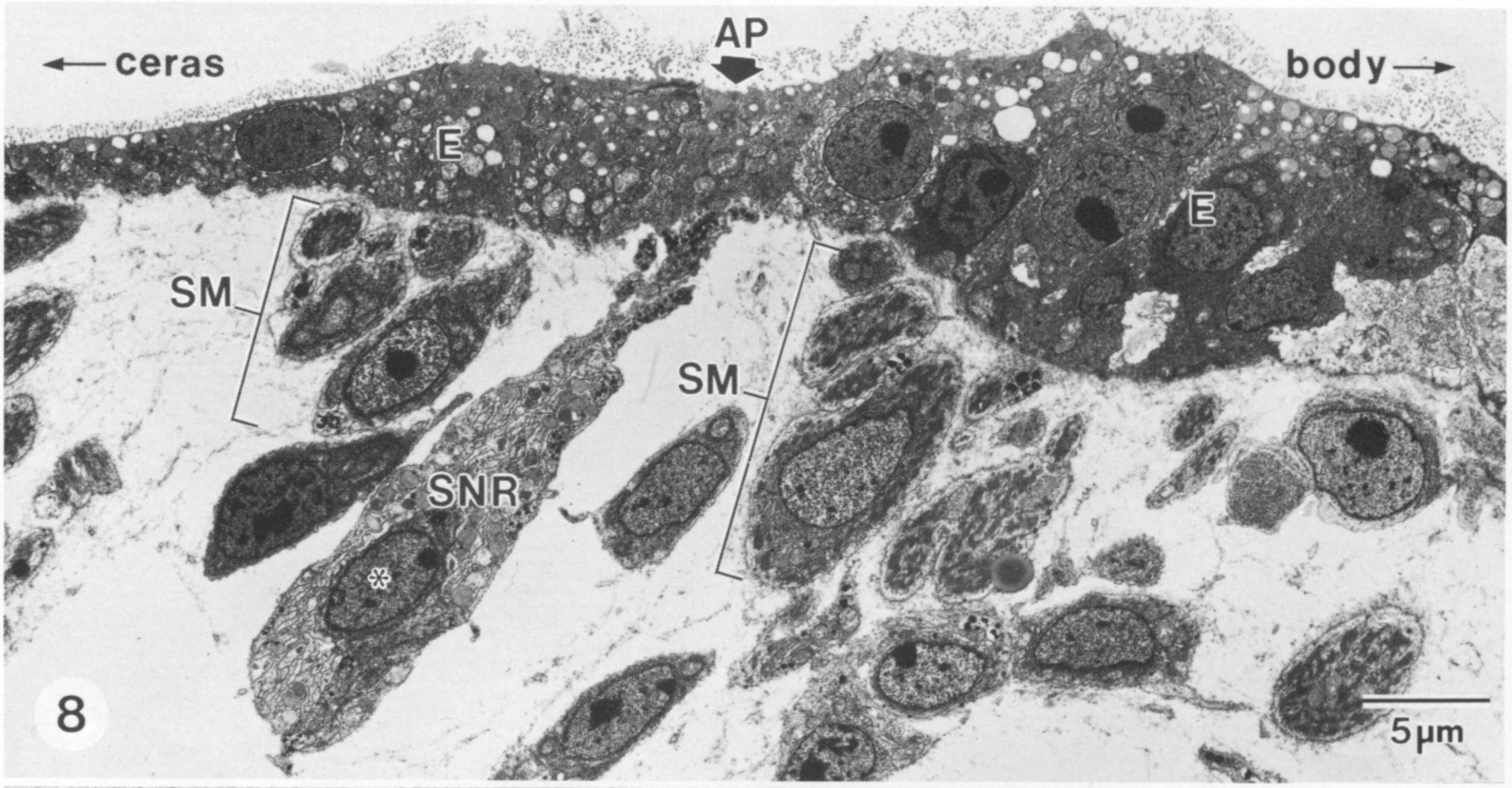

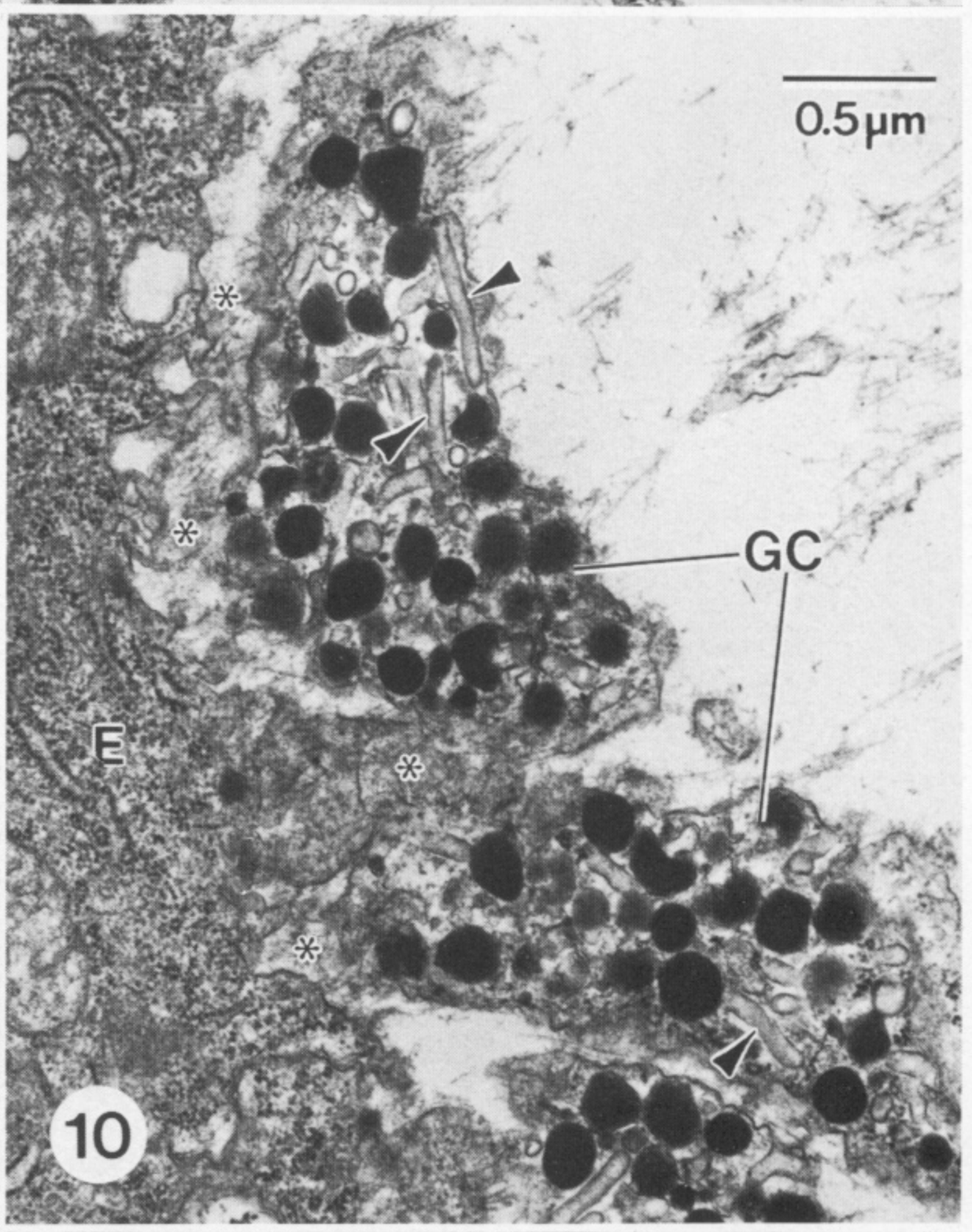

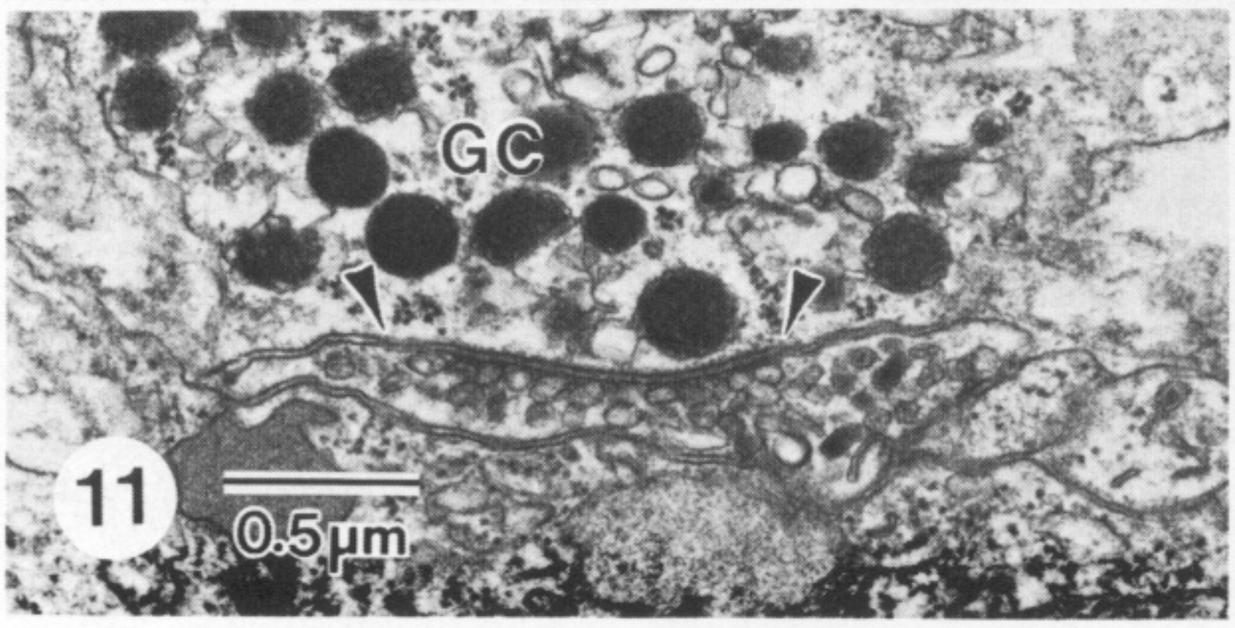

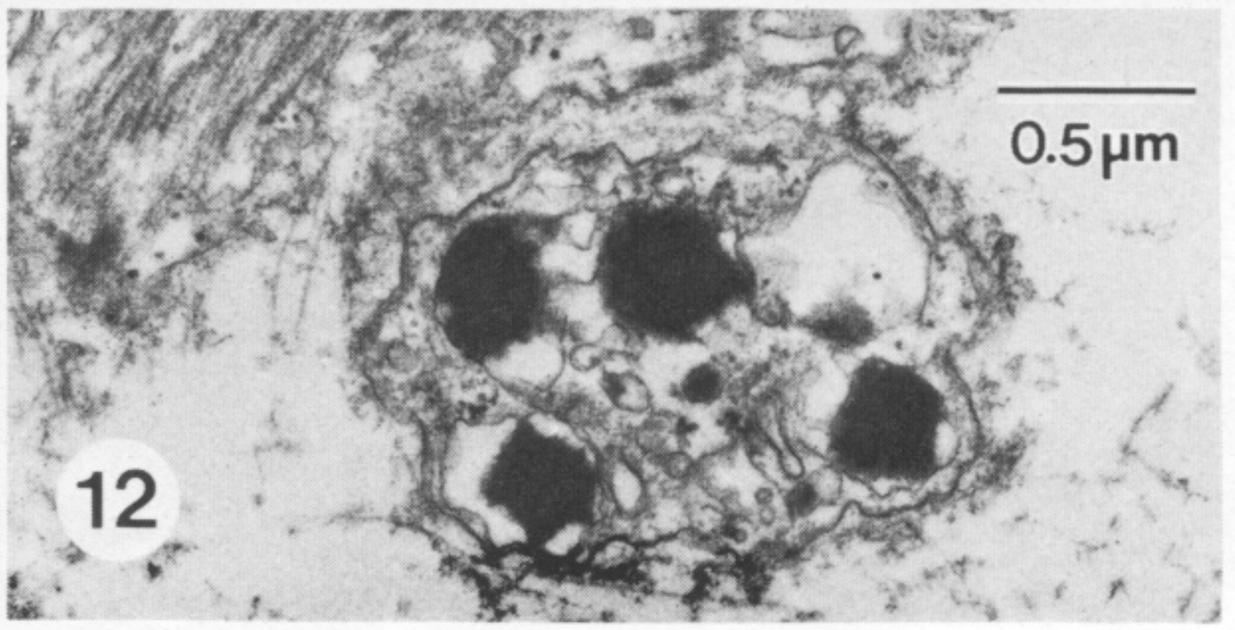

FIGURES 8–12. For description see p. 156.

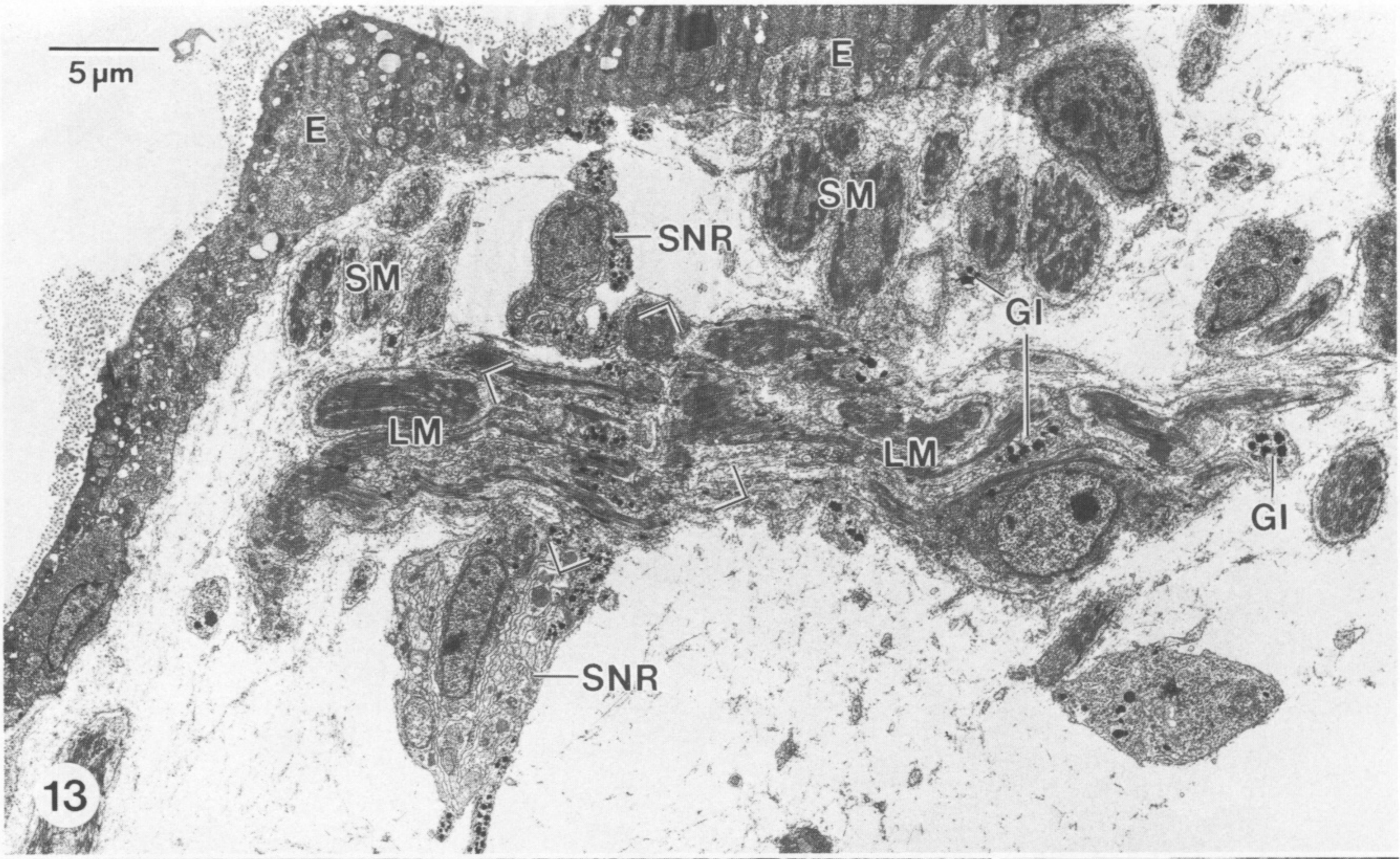

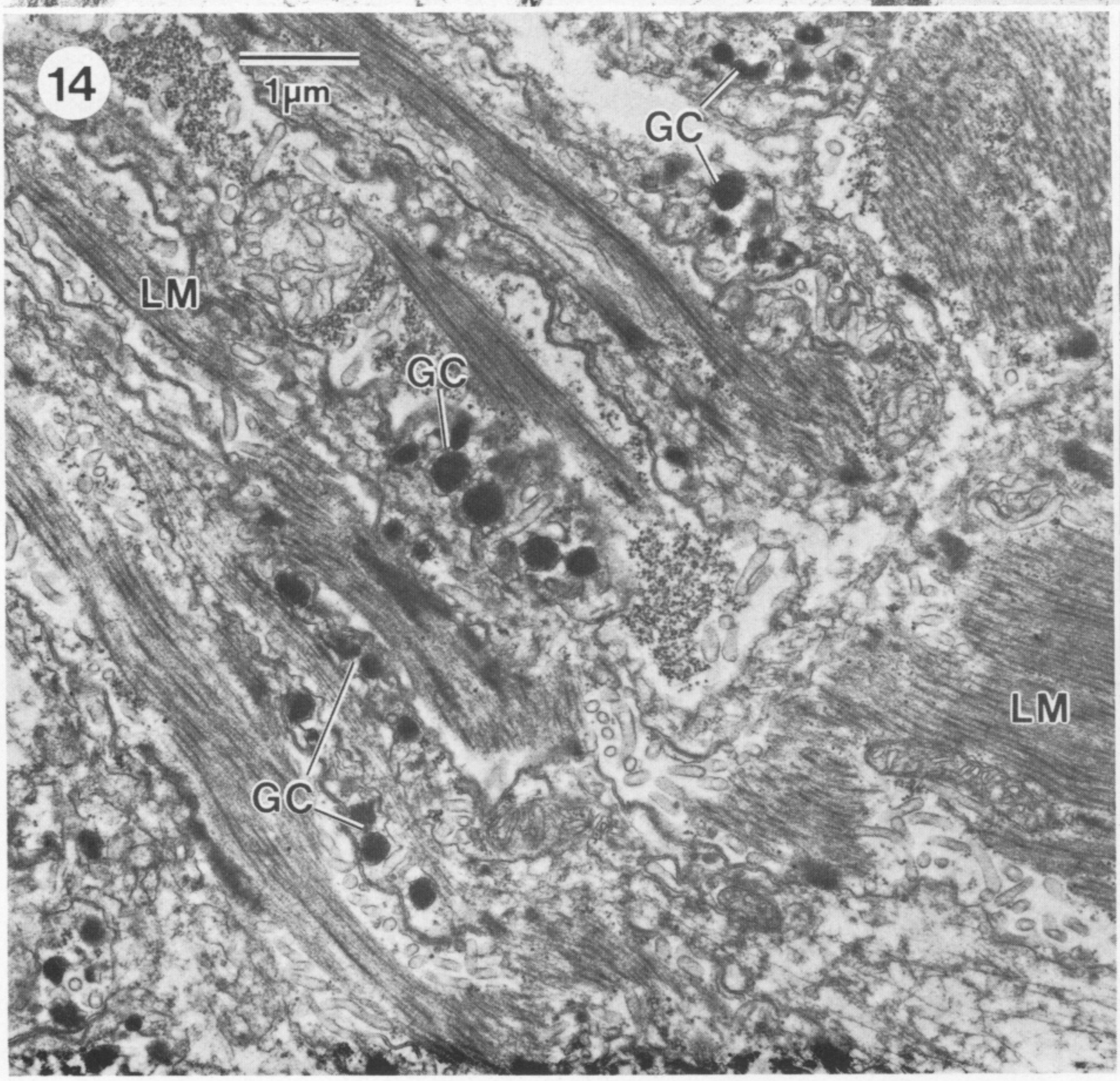

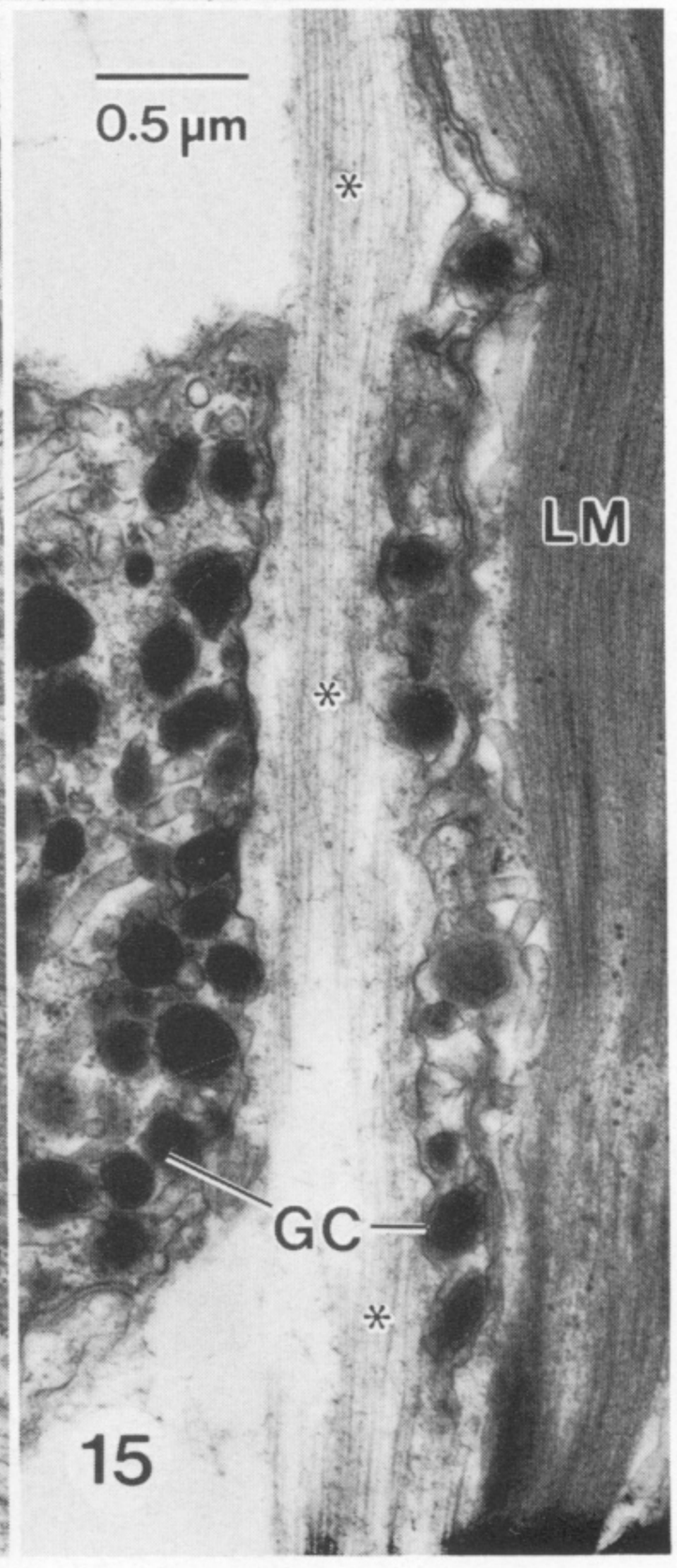

FIGURE 13. Longitudinal section through a longitudinal muscle band (LM) penetrating the subepidermal nerve ring (SNR). Epidermis (E); gliointerstitial cell processes (GI); subepidermal sphincter muscles (SM). Enlargement of bracketed area is shown in figure 14.

FIGURE 14. Cellular processes of granule-filled cells (GC) interdigitating with longitudinal-muscle fibres (LM) within the autotomy plane.

FIGURE 15. Detail of GC processes impinging onto a longitudinal-muscle fibre (LM) and associated connective tissue fibrils (asterisks).

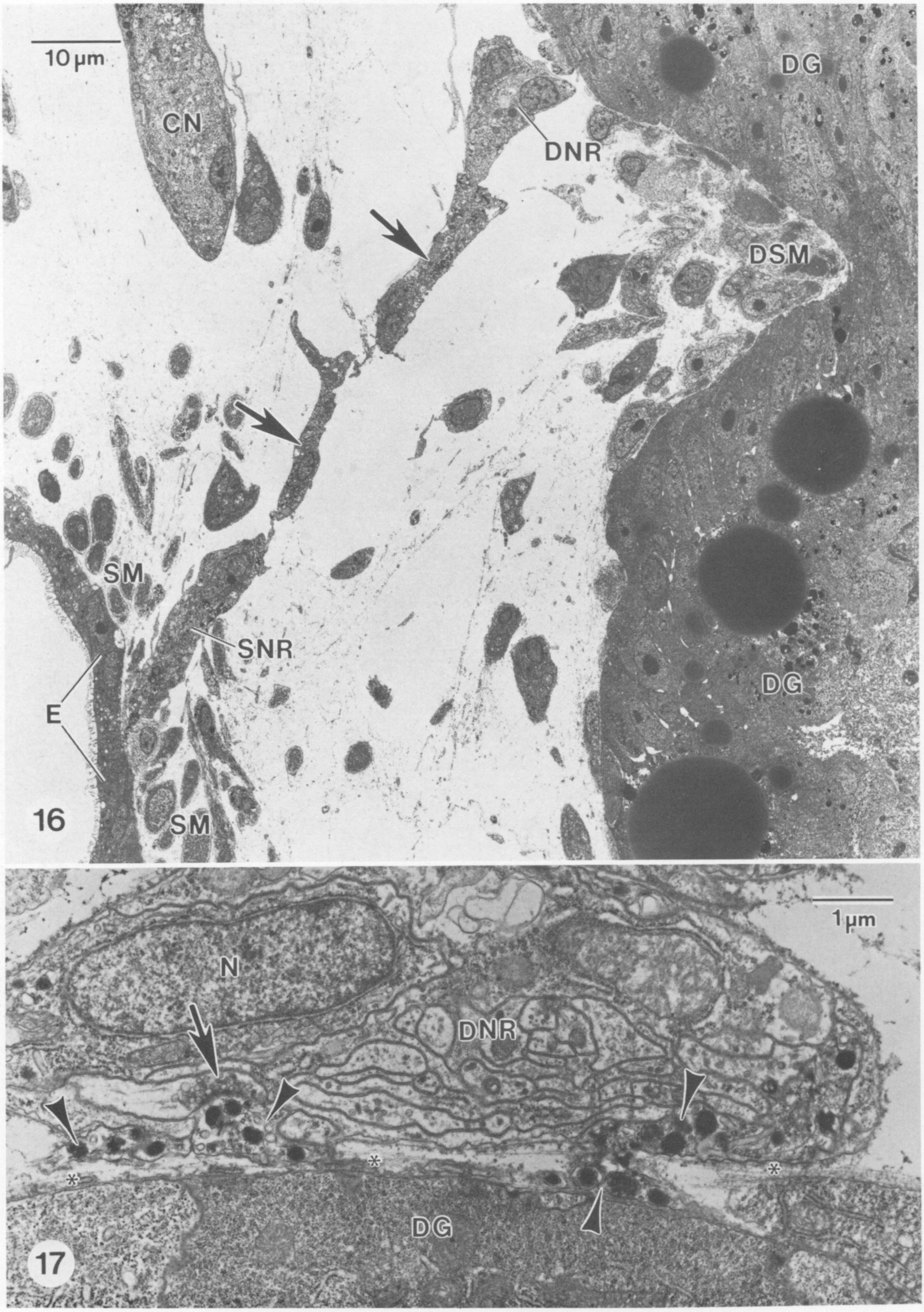

FIGURE 16. Longitudinal section through the ceratal autotomy plane showing one of the connectives (arrows) extending between the subepidermal nerve ring (SNR) and the digestive-gland nerve ring (DNR). Ceratal nerve (CN), digestive gland (DG), digestive-gland sphincter muscle (DSM), epidermis (E), subepidermal sphincter muscles (SM).

FIGURE 17. Cross section through the digestive gland nerve ring (DNR) showing the nucleus (N) of a GC and cellular processes of GC (arrowheads) impinging onto the basal lamina and connective tissue fibrils (asterisks) of the digestive gland (DG). The arrow indicates a synapse onto a GC process.

FIGURE 18. Oblique section through the ceratal nerve (CN) where it forms an anastomosis with a connective (CO) between the subepidermal nerve ring (SNR) and the digestive-gland nerve ring. Note the cell body of a GC. Epidermis (E).

FIGURE 19. Cytoplasmic processes of GC (large arrows) associated with the perineurium (small arrows) of the ceratal nerve (CN).

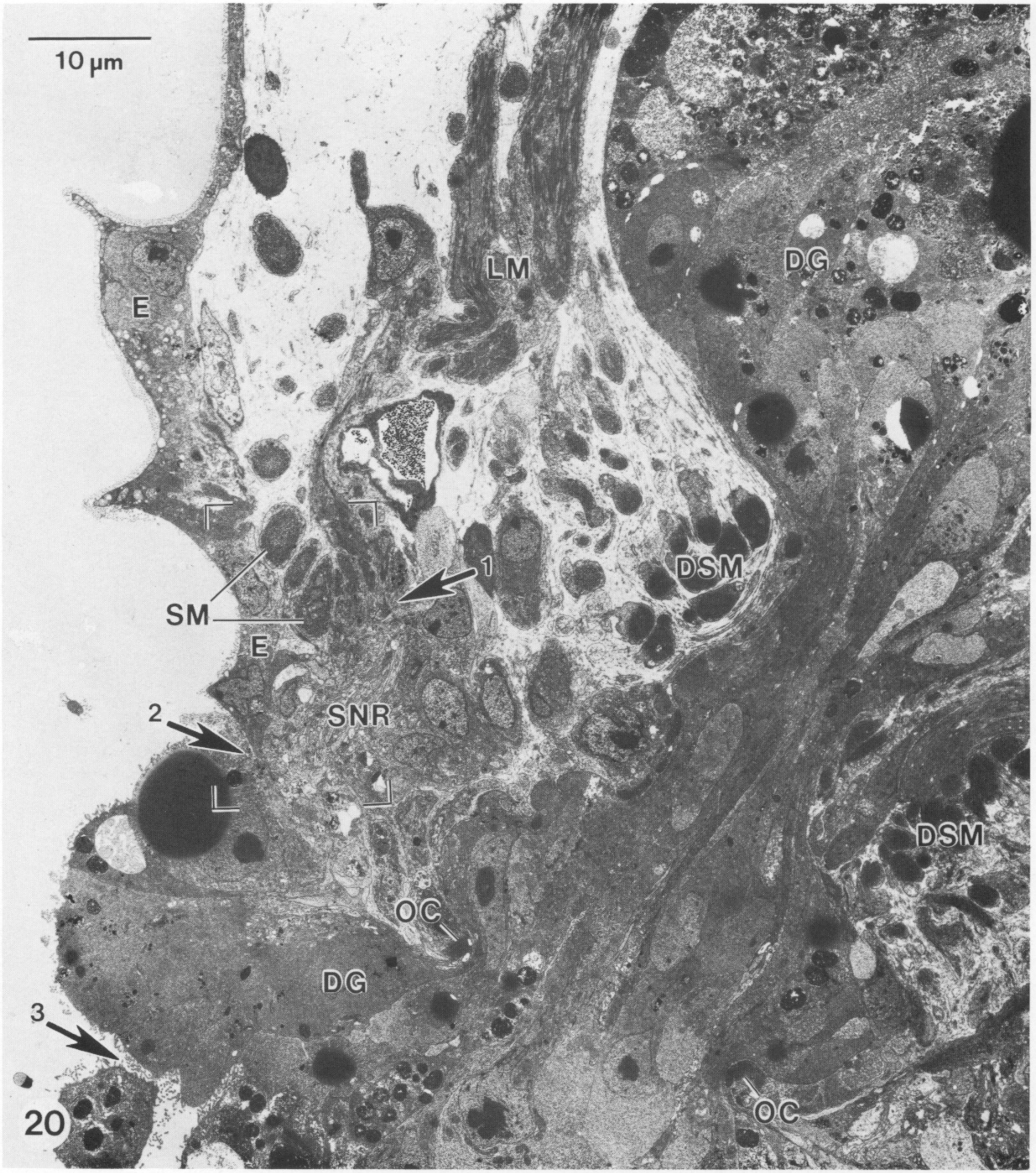

FIGURE 20. Longitudinal section through the base of an autotomized ceras. The broken ends of the longitudinal muscle bands (LM), epidermis (E), and digestive gland (DG) are indicated by arrows labelled 1, 2 and 3, respectively. Also note contracted digestive-gland sphincter (DSM), occasional circular muscles (OC), and subepidermal sphincter muscles (SM), and the subepidermal nerve ring (SNR). The bracketed area is enlarged in figure 21.

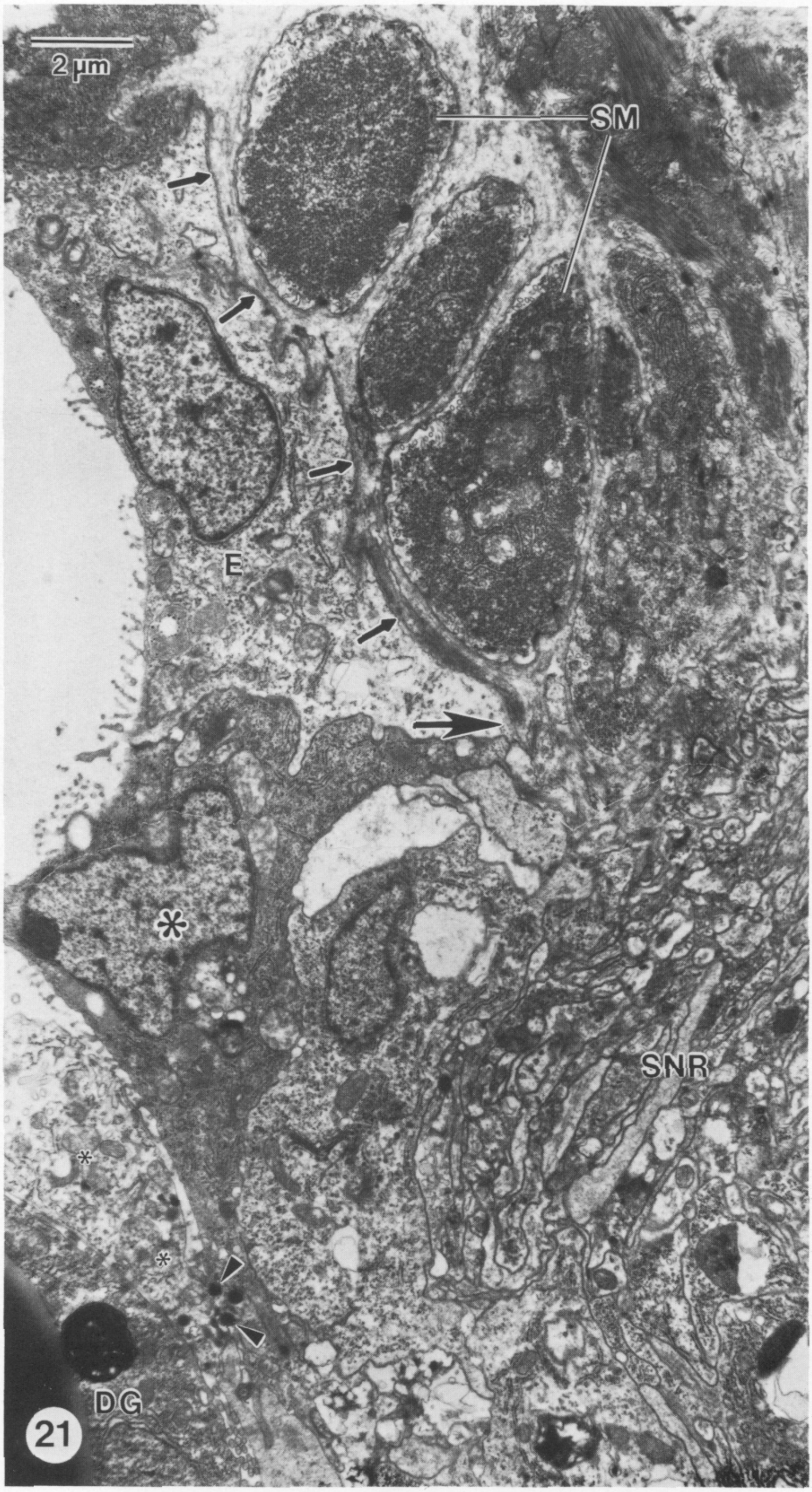

FIGURE 21. Longitudinal section through the epidermis (E) and subepidermal structures on the ceratal side of the autotomy plane of an autotomized ceras. Note the disruption (large arrow) of the epidermal basal lamina and associated connective-tissue fibrils (small arrows) just before the terminal epidermal cell (large asterisk) and the paucity of GC granules within the subepidermal nerve ring (SNR). Several granules (arrowheads) are present within a possible GC process (small asterisk) overlying the broken stump of the digestive gland (DG).

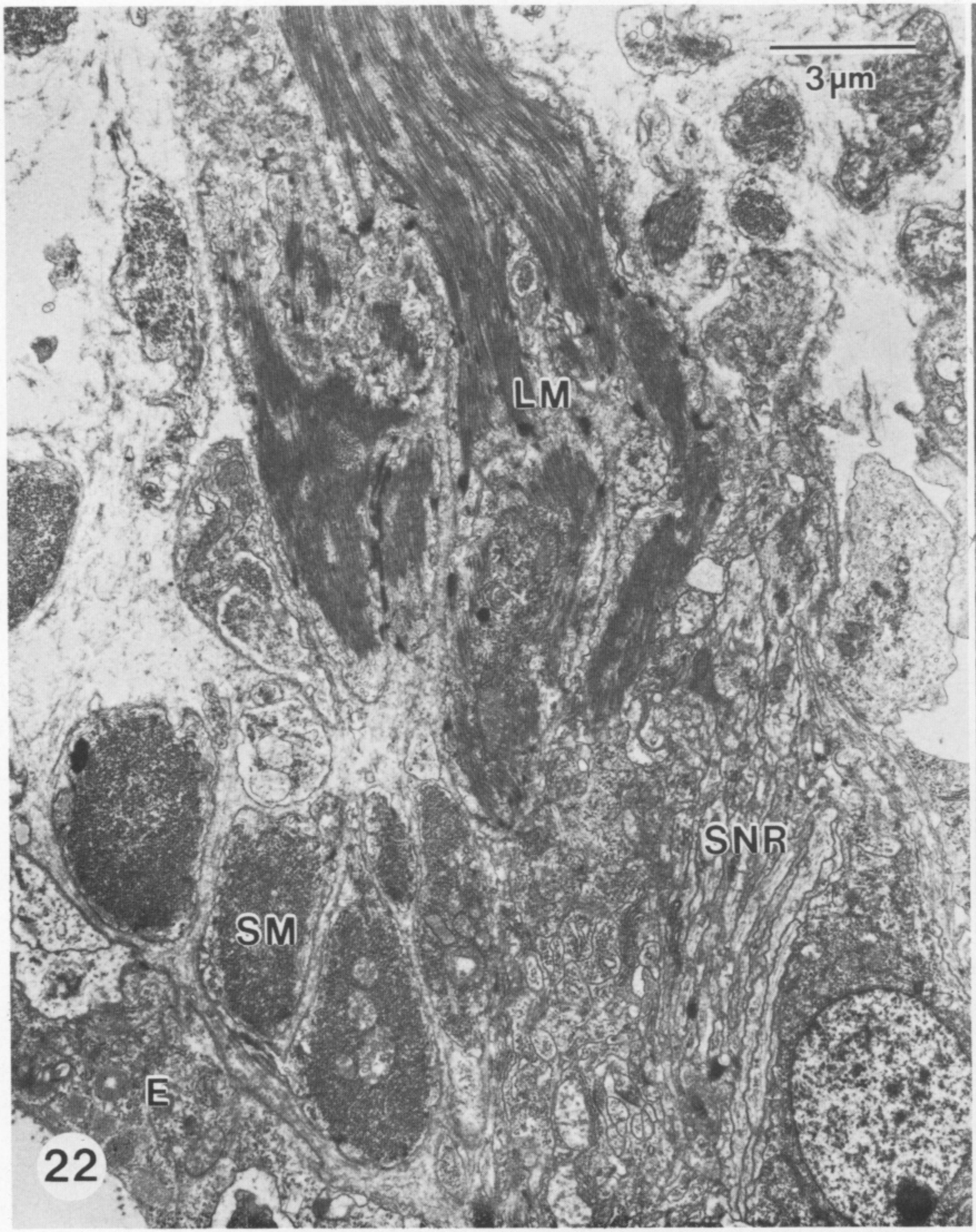

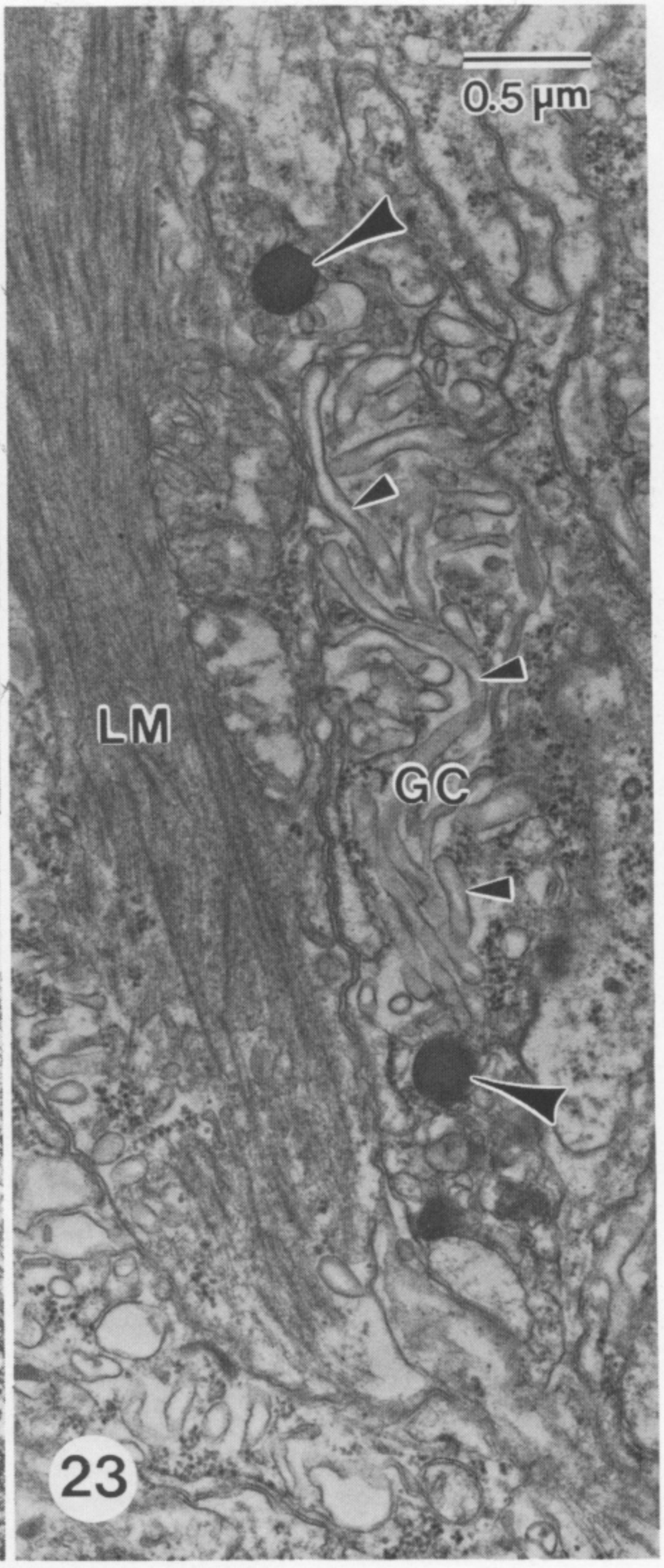

FIGURE 22. Longitudinal section through the base of an autotomized ceras showing the epidermis (E), subepidermal sphincter muscle (SM) and a longitudinal muscle band (LM). The LM is broken where it meets the subepidermal nerve ring (SNR).

FIGURE 23. Cellular process of a possible granule-filled cell (GC) adjacent to a terminal muscle fibre at the broken end of a longitudinal muscle band (LM). The process contains abundant smooth endoplasmic reticulum (small arrowheads) but few dense granules (large arrowheads).